

Rifampicin is a candidate preventive medicine against amyloid- β and tau oligomers

メタデータ	<p>言語: English</p> <p>出版者: Oxford University Press</p> <p>公開日: 2017-12-19</p> <p>キーワード: 神経変性疾患</p> <p>作成者: 梅田, 知宙, 小野, 賢二郎, 酒井, 亜由美, 山下, 港, 水口, 峰之, Klein, William L., 山田, 正仁, 森, 啓, 富山, 貴美</p> <p>メールアドレス:</p> <p>所属: Osaka City University, Japan Science and Technology Agency, Kanazawa University, Osaka City University, Osaka City University, University of Toyama, Northwestern University, Kanazawa University, Japan Science and Technology Agency, Osaka City University, Osaka City University, Japan Science and Technology Agency</p>
URL	<p>https://ocu-omu.repo.nii.ac.jp/records/2019690</p>

Rifampicin is a candidate preventive medicine against amyloid- β and tau oligomers

Tomohiro Umeda, Kenjiro Ono, Ayumi Sakai, Minato Yamashita,
Mineyuki Mizuguchi, William L. Klein, Masahito Yamada,
Hiroshi Mori and Takami Tomiyama

Citation	Brain, 139(5): 1568–1586,
Issue Date	2016-3-28
Type	Journal Article
Textversion	author
Rights	<p>This is a pre-copyedited, author-produced version of an article accepted for publication in <i>Brain</i> following peer review. The version of record Tomohiro Umeda, Kenjiro Ono, Ayumi Sakai, Minato Yamashita, Mineyuki Mizuguchi, William L. Klein, Masahito Yamada, Hiroshi Mori, Takami Tomiyama; Rifampicin is a candidate preventive medicine against amyloid-β and tau oligomers, <i>Brain</i>, Volume 139, Issue 5, 1 May 2016, Pages 1568–1586, is available online at: https://doi.org/10.1093/brain/aww042 .</p> <p>This is not the published version. Please cite only the published version.</p>
DOI	10.1093/brain/aww042

Self-Archiving by Author(s)
Placed on: Osaka City University Repository

Rifampicin is a candidate preventive medicine against amyloid β and tau oligomers

Running title: Prevention of dementia by rifampicin

Tomohiro Umeda, PhD,^{1,2} Kenjiro Ono, MD, PhD,^{3†} Ayumi Sakai, BSci,¹ Minato Yamashita, BSci,¹ Mineyuki Mizuguchi, PhD,⁴ William L. Klein, PhD,⁵ Masahito Yamada, MD, PhD,³ Hiroshi Mori, PhD,^{2,6} Takami Tomiyama, PhD^{1,2*}

¹ Department of Neuroscience, Osaka City University Graduate School of Medicine, Osaka, Japan.

² Core Research for Evolutional Science and Technology, Japan Science and Technology Agency, Kawaguchi, Japan.

³ Department of Neurology and Neurobiology and Aging, Kanazawa University Graduate School of Medical Science, Kanazawa, Japan.

⁴ Laboratory of Structural Biology, Graduate School of Medicine and Pharmaceutical Sciences, University of Toyama, Toyama, Japan.

⁵ Department of Neurobiology, Weinberg College of Arts and Science, Northwestern University, Evanston, IL, USA.

⁶ Department of Clinical Neuroscience, Osaka City University Medical School, Osaka, Japan.

[†] Present address: Department of Neurology, Showa University School of Medicine, Tokyo, Japan

*Corresponding author

Takami Tomiyama, PhD.

Department of Neuroscience, Osaka City University Graduate School of Medicine,

1-4-3 Asahimachi, Abeno-ku, Osaka 545-8585, Japan.

Phone: +81-6-6645-3921

FAX: +81-6-6645-3922

E-mail: tomi@med.osaka-cu.ac.jp.

Abstract

Amyloid β ($A\beta$), tau, and α -synuclein, or more specifically their soluble oligomers, are the etiologic molecules in Alzheimer's disease, tauopathies, and α -synucleinopathies, respectively. These proteins have been shown to interact to accelerate each other's pathology. Clinical studies of $A\beta$ -targeting therapies in Alzheimer's disease have revealed that the treatments after disease onset have little benefit on patient cognition. These findings prompted us to explore a preventive medicine which is orally available, has little adverse effects, and is effective at reducing neurotoxic oligomers with a broad spectrum. We initially tested five candidate compounds: rifampicin, curcumin, epigallocatechin-3-gallate, myricetin, and scyllo-inositol, in cells expressing amyloid precursor protein (APP) with the Osaka (E693 Δ) mutation, which promotes $A\beta$ oligomerization. Among these compounds, rifampicin, a well-known antibiotic, showed the strongest activities against the accumulation and toxicity (i.e. cytochrome c release from mitochondria) of intracellular $A\beta$ oligomers. Under cell-free conditions, rifampicin inhibited oligomer formation of $A\beta$, tau, and α -synuclein, indicating its broad spectrum. The inhibitory effects of rifampicin against $A\beta$ and tau oligomers were evaluated in APP_{OSK} mice ($A\beta$ oligomer model), Tg2576 mice (Alzheimer's disease model), and tau609 mice (tauopathy model). When orally administered to 17-month-old APP_{OSK} mice at 0.5 and 1 mg/day for 1 month, rifampicin reduced the accumulation of $A\beta$ oligomers as well as tau hyperphosphorylation, synapse loss, and microglial activation in a dose-dependent manner. In the Morris water maze, rifampicin at 1 mg/day improved memory of the mice to a level similar to that in non-Tg littermates. Rifampicin also inhibited cytochrome c release from the mitochondria and caspase-3 activation in the hippocampus. In 13-month-old Tg2576 mice, oral rifampicin at 0.5

mg/day for 1 month decreased A β oligomer accumulation, tau hyperphosphorylation, synapse loss, and microglial activation, but not amyloid deposition. Rifampicin treatment to 14-15-month-old tau609 mice at 0.5 and 1 mg/day for 1 month also reduced tau oligomer accumulation, tau hyperphosphorylation, synapse loss, and microglial activation in a dose-dependent fashion, and improved the memory almost completely at 1 mg/day. In addition, rifampicin decreased the level of p62/sequestosome-1 in the brain without affecting the increased levels of LC3 (microtubule-associated protein light chain 3) conversion, suggesting the restoration of autophagy-lysosomal function. Considering its prescribed dose and safety in humans, these results indicate that rifampicin could be a promising, ready-to-use medicine for the prevention of Alzheimer's disease and other neurodegenerative diseases.

Keywords:

Neurodegenerative disease; prevention; oligomer; mitochondria; autophagy

Abbreviations:

A β = amyloid β ; APP = amyloid precursor protein; BBB = blood-brain barrier; CMC = carboxyl methyl cellulose; CTF = carboxyl terminal fragment; DMSO = dimethyl sulfoxide; DTT = dithiothreitol; EGCG = epigallocatechin-3-gallate; ELISA = enzyme-linked immunosorbent assay; ER = endoplasmic reticulum; FA = formic acid; FITC = fluorescein isothiocyanate; FTDP-17 = frontotemporal dementia and parkinsonism linked to chromosome 17; GST = glutathione-S-transferase; GuHCl = guanidine hydrochloride; HSQC = heteronuclear single quantum coherence; LC3 = microtubule-associated protein light chain 3; MALDI-TOF MS = matrix assisted laser

desorption/ionization-time of flight mass spectrometry; NMR = nuclear magnetic resonance; PICUP = photo-induced cross-linking of unmodified proteins; ROS = reactive oxygen species; SDS-PAGE = sodium dodecyl sulfate polyacrylamide gel electrophoresis; SQSTM1 = sequestosome-1; TBS = Tris-buffered saline

Introduction

Neurodegenerative diseases are characterized by the accumulation of insoluble aggregates of misfolded proteins in the CNS. For example, Alzheimer's disease shows extracellular deposits of amyloid β ($A\beta$) aggregates and intracellular inclusions of hyperphosphorylated tau aggregates. Intracellular tau inclusions are also a hallmark of tauopathies (Lee et al., 2001), which include Pick's disease, corticobasal degeneration, progressive supranuclear palsy, argyrophilic grain disease, and frontotemporal dementia and parkinsonism linked to chromosome 17 (FTDP-17). A different type of neurodegenerative disorders, α -synucleinopathies (Galvin et al., 2001), which include diffuse Lewy body disease, Parkinson's disease, and multiple system atrophy, exhibits intracellular inclusions of α -synuclein aggregates. Recent evidence suggests that these proteins aggregate, more specifically their soluble oligomers, impair synaptic and cognitive function (Lambert et al., 1998; Walsh et al., 2002; Cleary et al., 2005; Diógenes et al., 2012; Lasagna-Reeves et al., 2012; Martin et al., 2012) and mediate the cell-to-cell propagation of neuropathology (Danzer et al., 2009; Langer et al., 2011; Lasagna-Reeves et al., 2012). Thus, reducing neurotoxic oligomers would appear to be a rational strategy to treat these diseases.

Clinical studies of $A\beta$ -targeting therapies in Alzheimer's disease have revealed that the treatments after disease onset have little effect on the cognition of patients (Imbimbo and Giardina, 2011; Panza et al., 2014). In addition, $A\beta$, tau, and α -synuclein have been shown to synergistically interact to accelerate each other's pathology (Clinton et al., 2010; Larson et al., 2012; Umeda et al., 2014). These findings suggest that the treatment of neurodegenerative diseases should be started prior to the onset of clinical symptoms (Sperling et al., 2011) and that not only the etiologic molecule but also other

associated proteins should be targeted together, desirably with one drug. This notion prompted us to develop a preventive medicine which is orally available, has little adverse effects, and is effective at reducing extracellular and intracellular neurotoxic oligomers with a broad spectrum.

To explore such drugs, we consulted the literature for natural and semi-natural small compounds that have inhibitory activity against A β aggregation. Natural small compounds are presumed to have less adverse effects and are cheaper for long-term preventive treatment. We selected five compounds as candidates: rifampicin (Tomiyama et al., 1994, 1996, 1997), curcumin (Lim et al., 2001; Ono et al., 2004; Yang et al., 2005), epigallocatechin-3-gallate (EGCG) (Bastianetto et al., 2006; Rezai-Zadeh et al., 2008), myricetin (Ono et al., 2003; Hamaguchi et al., 2009), and scyllo-inositol (McLaurin et al., 2000, 2006). These compounds have been shown to interact with A β to affect its aggregation in vitro and, except rifampicin, ameliorate amyloid pathology in mouse models when orally administered. Rifampicin is a well-known antibiotic used in humans and is known to penetrate into the brain following oral administration (No authors, 2008). Among these candidates, we found that rifampicin had the strongest activities against the accumulation and toxicity of intracellular A β oligomers in cultured cells. Under cell-free conditions, rifampicin inhibited the oligomer formation of A β , tau, and α -synuclein, indicating its broad spectrum. When orally administered to three different mouse models of Alzheimer's disease and tauopathy, rifampicin reduced the accumulation of A β oligomers and tau oligomers, respectively, and improved the memory of the mice. Our results indicate that rifampicin could be a promising, ready-to-use medicine for the prevention of Alzheimer's disease and other neurodegenerative diseases.

Materials and methods

Immunocytochemical analysis of A β oligomers in cultured cells

Rifampicin, myricetin, and EGCG were purchased from Sigma-Aldrich (St. Louis, MO), and curcumin and scyllo-inositol were purchased from Wako Pure Chemical Industries (Osaka, Japan) and Tokyo Chemical Industry (Tokyo, Japan), respectively. The stock solutions of rifampicin, myricetin, and EGCG were prepared at 100 mM in DMSO, while that of curcumin was at 10 mM in ethanol and that of scyllo-inositol was at 1 mM in OPTI-MEM I medium (Life Technologies, Carlsbad, CA). COS-7 cells cultured in OPTI-MEM I medium were transfected with APP_{OSK} construct using the Lipofectamine Plus reagent (Invitrogen, Carlsbad, CA), as described previously ([Umeda et al., 2011](#)). On the day after the transfection, each compound was added to the culture to a final concentration of 100 μ M. The cells were further cultured for 2 days, and then fixed with 4% paraformaldehyde and treated with 0.05% Tween-20, as described previously ([Umeda et al., 2011](#)). The cells were stained with A β oligomer-selective NU-1 antibody ([Lambert et al., 2007](#)) followed by FITC-labelled anti-mouse IgG antibody (Jackson ImmunoResearch Laboratories, West Grove, PA) and counterstained with DAPI (Molecular Probes, Eugene, OR). FITC fluorescence intensity in a constant field (400 μ m \times 400 μ m) of the culture was quantified using NIH ImageJ software, and the number of DAPI-positive cells in the same field was counted. A β oligomer accumulation was assessed by dividing the FITC intensity with the cell number.

Biochemical analysis of A β oligomers in cultured cells

COS-7 cells transfected with APP_{OSK} construct were treated with rifampicin at 100 μ M for 2 days, as described above. Conditioned media were collected for A β ELISA. Cells in a 10-cm dish were harvested and lysed by sonication in 100 μ l of 1% Triton X-100 in 50 mM Tris-HCl, pH 7.6, and 150 mM NaCl (TBS) containing 1/100 volumes of protease inhibitor cocktail (P8340; Sigma-Aldrich). The cell lysates were subjected to Western blot with mouse monoclonal 82E1 antibody (IBL, Fujioka, Japan) for A β , rabbit polyclonal C40 antibody (Tomiyama et al., 2010) for APP, and rabbit polyclonal anti-actin antibody (Sigma-Aldrich). Signals were visualized using an LAS-3000 luminescent image analyzer (Fujifilm, Tokyo, Japan). The levels of A β ₄₀, A β ₄₂, and A β oligomers in conditioned media were measured using Human β Amyloid(1-40) ELISA kit Wako II; Human β Amyloid(1-42) ELISA kit Wako, High-sensitive (both from Wako); and Human Amyloid β Oligomers (81E1-specific) Assay kit-IBL (IBL), respectively.

Photo-induced cross-linking of unmodified proteins (PICUP) assay

Synthetic A β ₄₀ and A β ₄₂ peptides (Peptide Institute, Mino, Japan) were dissolved to 50 μ M in 10% (v/v) 60 mM NaOH and 90% (v/v) 10 mM phosphate buffer, pH 7.4.

Recombinant tau-441 protein (rPeptide, Bogart, GA) was dissolved to 50 μ M in 20 mM Tris buffer, pH 7.4, while recombinant α -synuclein protein (rPeptide) was dissolved to 50 μ M in 10 mM HEPES buffer, pH 7.4. After sonication for 1 min, these protein solutions were centrifuged for 10 min at 16,000 \times g. A stock solution of glutathione-S-transferase (GST; Sigma-Aldrich) was prepared by dissolving the lyophilizate to a concentration of 250 μ M in 60 mM NaOH. Prior to use, the GST solution was diluted to 50 μ M with 10 mM phosphate buffer, pH 7.4. Rifampicin

(Sigma-Aldrich) was dissolved to 2.5 mM in ethanol and then diluted to 50 and 200 μ M with 10 mM phosphate buffer, pH 7.4. The protein solutions were mixed with the rifampicin solutions at 1:1 volume and immediately cross-linked by PICUP, as described previously (Ono et al., 2009, 2012). The samples were subjected to SDS-PAGE with 10-20% Tricine gels under reducing conditions, and the oligomer formation of each protein was visualized by silver staining using the SilverQuest Silver Staining Kit (Invitrogen).

To confirm the PICUP results, A β oligomers were measured by ELISA. A β 42 peptide with the Osaka mutation (Peptide Institute) was dissolved to 500 μ M in 60 mM NaOH and diluted to 25 μ M in PBS containing rifampicin at 25 μ M or 100 μ M. The mixtures were subjected to sandwich A β 42 ELISA (Wako) and direct oligomer ELISA (see below).

Rifampicin treatment of model mice

Rifampicin was dissolved by sonication to 1 and 2 mg/ml in 0.5% low-viscosity carboxyl methyl cellulose (CMC; Sigma-Aldrich) just before use every day. 500 μ l of either rifampicin solution was orally administered using feeding needles to male APP_{OSK} mice, Tg2576 mice (Taconic, Hudson, NY), and tau609 mice (n = 6-12 per group) every day for 1 month. Age-matched Tg and non-Tg littermates (n = 6-17 per group) administered CMC solution without rifampicin were used as controls. All animal experiments were approved by the ethics committee of Osaka City University (Osaka, Japan) and performed in accordance with the Guide for Animal Experimentation, Osaka City University.

Behavioral test of model mice

Spatial reference memory in mice was examined using the Morris water maze, as described previously (Umeda et al., 2013, 2015). The tests were performed under unblinded conditions: the experimenter knew which mice were treated with rifampicin. Daily oral administration of rifampicin was continued during the behavioral test.

Immunohistochemical analysis of amyloid and tau pathologies in model mice

After the behavioral tests, brain sections were prepared and immunohistochemical staining was performed as described previously (Umeda et al., 2014, 2015). For APP_{OSK} mice, A β oligomers and phosphorylated tau were stained with mouse monoclonal 11A1 (IBL) and PHF-1 antibodies (a kind gift from Dr. Peter Davies, Albert Einstein College of Medicine), respectively. For Tg2576 mice, amyloid deposits were stained with those antibodies and rabbit polyclonal β 001 antibody (Tomiyama et al., 2010). For tau609 mice, tau oligomers and phosphorylated tau were stained with rabbit polyclonal T22 antibody (EMD Millipore, Temecula, CA) and mouse monoclonal PHF-1, AT8 (Thermo Scientific, Waltham, MA), and Ta1505 antibodies (Umeda et al., 2015), respectively. Synaptophysin and microglia were stained with mouse monoclonal antibody to synaptophysin (SVP-38; Sigma-Aldrich) and rabbit polyclonal antibody to Iba-1 (Wako Pure Chemical Industries), respectively. Amyloid deposition, A β oligomer accumulation, tau oligomer accumulation, tau hyperphosphorylation, synapse loss, and microglial activation were evaluated by quantifying the corresponding antibody-staining areas/intensities per unit area in each photograph using NIH ImageJ software, as described previously (Umeda et al., 2014; 2015).

Biochemical analysis of amyloid and tau pathologies in model mice

Hippocampal tissues were dissected from mouse brains and homogenized by sonication in 4 volumes of TBS containing protease inhibitor cocktail (P8340). The homogenates were subjected to Western blot with SVP-38 antibody for synaptophysin and anti-actin antibody. The remaining brain tissues, not including the cerebellum, were homogenized in 4 volumes of TBS containing P8340, along with phosphatase inhibitor cocktail (Nacalai Tesque, Kyoto, Japan) for tau609 mice, using a tissue grinder with Teflon pestle. The homogenates were subjected to Western blot with C40 antibody and mouse monoclonal 6E10 antibody (Covance, Princeton, NJ) for total and human APP, respectively; and rabbit polyclonal pool-2 antibody (Umeda et al., 2013) and mouse monoclonal Tau12 antibody (Abcam, Cambridge, UK) for total and human tau, respectively.

Brain homogenates from APP_{OSK} and Tg2576 mice were fractionated by three-step ultracentrifugation including TBS, 2% SDS, and 70% formic acid (FA) extraction, essentially as described previously (Tomiyama et al., 2010). A portion of SDS and FA extracts were dialyzed against TBS at 4 °C overnight using Slide-A-Lyzer Dialysis Cassette G2 with 2K cut-off membrane (Thermo Scientific). The levels of A β 40, A β 42, and A β oligomers in each fraction were measured using the corresponding ELISA kits. Dialyzed SDS extracts were used only for oligomer ELISA, whereas dialyzed FA extracts were used for all ELISA. For the measurement of A β 40 and A β 42 in APP_{OSK} samples, synthetic peptides with the Osaka (E22 Δ) mutation (American Peptide Company, Sunnyvale, CA) were used as standards. The levels of A β oligomers were also quantified by direct ELISA with 11A1 antibody (at 1 μ g/ml) according to the method of Castillo-Carranza et al. (2015), except that each fraction was diluted 2-fold in

0.05 M sodium bicarbonate and allowed to coat ELISA plates at 50 μ l/well. On the other hand, brain homogenates from tau609 mice were fractionated by three-step ultracentrifugation including TBS, 1% N-lauroylsarcosinate (sarkosyl), and 4 M guanidine hydrochloride (GuHCl) extraction, essentially as described previously (Umeda et al., 2013). GuHCl extracts were dialyzed against TBS at 4 °C overnight using Slide-A-Lyzer Dialysis Cassette G2 with 20K cut-off membrane (Thermo Scientific). The levels of human tau, pSer396-tau, and pSer199-tau in each fraction were measured using TAU (total) ELISA kit, Human; TAU [pS396] Human ELISA kit; and TAU [pS199] Phospho-ELISA kit, Human (all from Novex, Thermo Scientific), respectively. The levels of tau oligomers were quantified by direct ELISA with T22 antibody (1:250) according to the method of Castillo-Carranza et al. (2015), as described above.

Statistical analysis

Comparisons of means among more than two groups were performed using ANOVA or two-factor repeated measures ANOVA (for the behavioral tests), followed by Fisher's PLSD test. Differences with a *p* value of < 0.05 were considered significant.

Results

Effects of candidate compounds on intracellular A β oligomers in cultured cells

A recent study using iPS cells derived from patients with Alzheimer's disease suggests that Alzheimer's disease can be classified into two categories: extracellular A β type and intracellular A β type (Kondo et al., 2013). This finding indicates that it is desirable for A β -targeting medicines to penetrate into cells. The Osaka mutation in APP has been

shown to cause an intraneuronal accumulation of A β oligomers (Tomiyama et al., 2008, 2010; Nishitsuji et al. 2009; Umeda et al., 2011), and thus provides a good model for study of the intracellular A β type. We examined the effects of five candidate compounds: rifampicin, curcumin, EGCG, myricetin, and scyllo-inositol, on the accumulation of intracellular A β oligomers in APP_{OSK}-expressing cells. COS-7 cells transfected with APP_{OSK} were cultured for 2 days in the presence of each compound at 100 μ M and stained with A β oligomer-selective NU-1 antibody. All compounds decreased NU-1-positive staining, with rifampicin having the highest activity and myricetin the lowest (Fig. 1A, B). Western blot with cell homogenates revealed that rifampicin significantly reduced the levels of intracellular A β dimers and possible trimers and tended to decrease A β monomers without affecting APP expression (Fig. 1C, D). Simultaneously, conditioned media of rifampicin-treated cells were collected and subjected to ELISA to measure A β ₄₀, A β ₄₂, and A β oligomers. Rifampicin significantly increased extracellular levels of A β ₄₀ and A β ₄₂ and significantly decreased A β oligomers (Fig. 1E-G). We observed that rifampicin did not affect A β production from full-length APP or its β -cut fragment in cultured cells (Supplementary Fig. 1). Taken together, these results suggest that rifampicin inhibits intracellular and extracellular A β (particularly A β ₄₂) oligomerization and promotes the secretion of A β monomers from cells.

We also compared the protective effects of the five compounds against intracellular A β -induced cell damage. Transfected cells treated with each compound at 1-100 μ M for 2 days were harvested, and the level of cytochrome c released from the mitochondria into the cytoplasm was measured by Western blot. All compounds reduced the level of cytosolic cytochrome c in a dose-dependent manner, with

rifampicin and curcumin having the highest activity and scyllo-inositol the lowest (Supplementary Fig. 2). Thus, rifampicin showed the strongest protective effects on the accumulation and toxicity of intracellular A β oligomers. Since rifampicin has long been used in humans as an antibiotic without serious adverse effects, we chose rifampicin as a favorable candidate for preventive medicine and subjected it to further evaluation.

Effects of rifampicin on protein oligomerization under cell-free conditions

We examined the effects of rifampicin on the oligomer formation of A β , tau, and α -synuclein under cell-free conditions. Synthetic A β 40 and A β 42 peptides were incubated in the presence of rifampicin at a molar ratio of 1:1 and 1:4 and cross-linked by the PICUP method. Rifampicin inhibited the oligomer formation of both A β 40 and A β 42 peptides in a dose-dependent manner with complete inhibition of A β 40 oligomerization at the ratio 1:4 (Fig. 2A, B). Similar experiments were performed using recombinant tau-441 and α -synuclein proteins, with GST as the control. Again, rifampicin inhibited the oligomer formation of tau and α -synuclein in a dose-dependent manner, with almost complete inhibition at the ratio 1:4 (Fig. 2C, D). No effect was seen with GST (Fig. 2E). The result for A β 42 was confirmed by ELISA using synthetic A β 42 peptide with the Osaka mutation. Rifampicin decreased the levels of A β oligomers (Fig. 2F) and inversely increased the levels of A β 42 (probably monomers) in the peptide solutions in a dose-dependent manner (Fig. 2G).

To investigate the mechanism by which rifampicin inhibits oligomer formation of neuropathogenic proteins but not GST, we analyzed the interaction of rifampicin with A β 42, tau-441, α -synuclein, and GST by nuclear magnetic resonance (NMR) spectroscopy. NMR spectroscopy cannot detect heterogeneous, minor species, such as

oligomers in the protein solutions, and thus provides information primarily on monomers. When incubated with these proteins, rifampicin caused neither chemical shift changes nor line broadening (Supplementary Fig. 3), suggesting that rifampicin does not bind to the protein monomers. A β , tau, and α -synuclein are known to take the β -sheet structure during aggregation into fibrils (Tomiyama et al., 1996; Li et al., 2004; von Bergen et al., 2005). We considered whether rifampicin binds to only protein oligomers that grow to amyloid fibrils taking extended β -sheet structure, which would suggest GST oligomers do not. To test this theory, we performed thioflavin T assays, in which the fluorescence intensity reflects the levels of β -sheet structure primarily in high-order protein assemblies such as fibrils. A β 42 peptide at 25 μ M showed an increase in fluorescence intensity during incubation, whereas GST at the same concentration did not (Supplementary Fig. 4). Taken together with the findings in Figs. 1C-G and 2F-G, these results suggest that rifampicin binds to a certain conformation (for example, extended β -sheet) of amyloidogenic protein oligomers that is not formed in physiological oligomers of non-amyloidogenic proteins, in order to promote their dissociation into monomers. Thus, rifampicin was shown to have anti-oligomerizing activity with a broad spectrum but specific to amyloidogenic proteins.

Effects of rifampicin on memory and A β oligomers in APP_{OSK} mice

APP_{OSK} mice are a transgenic mouse model of Alzheimer's disease that accumulate A β oligomers without forming amyloid plaques (Tomiyama et al., 2010). The mice exhibit intraneuronal accumulation of A β oligomers and subsequent tau hyperphosphorylation, synapse loss, and memory impairment at 8 months, microglial activation at 12 months, and neuronal loss at 24 months. Thus, APP_{OSK} mice are an ideal model for investigating

the effects of rifampicin on A β oligomers in vivo. Rifampicin is usually prescribed to adult humans at 10 mg/kg daily (No authors, 2008). Assuming a mean body weight of adult mice of 30 g, the mean dose for mice corresponds to 0.3 mg daily. We decided the daily dose of rifampicin for mice as 0.5 mg. Rifampicin dissolved in 0.5% CMC was orally administered to 11-12-month-old APP_{OSK} mice (mean body weight 35.5 g) at 0.5 mg/shot every day for 1 month. The spatial reference memory of mice was examined using the Morris water maze. Compared with CMC-treated age-matched non-Tg littermates, CMC-treated Tg mice showed significantly impaired memory, whereas rifampicin-treated Tg mice exhibited a significant improvement of memory to almost the same level (Fig. 3A, B). We repeated the experiment using older APP_{OSK} mice. Rifampicin was administered to 17-month-old APP_{OSK} mice (mean body weight 37.8 g) at 0.5 and 1 mg/shot every day for 1 month. In the Morris water maze, rifampicin restored the memory of Tg mice in a dose-dependent fashion. The memory of Tg mice was markedly improved by 1 mg/shot of rifampicin to a level similar to that in non-Tg littermates and significantly but to a lesser degree at 0.5 mg/shot (Fig. 3C, D).

Brain sections were prepared from 18-month-old rifampicin-treated mice and stained with A β oligomer-specific 11A1 antibody. Rifampicin significantly reduced 11A1-positive staining in the cerebral cortex and hippocampus in a dose-dependent manner (Fig. 4A, B, and Supplementary Fig. 5A). Brain homogenates were prepared from 18-month-old rifampicin-treated mice (at 1 mg/day) and separated into TBS-, SDS-, and FA-soluble fractions. Western blot with brain homogenates revealed no significant differences in the levels of total (C40-positive) and human APP (6E10-positive) between CMC- and rifampicin-treated Tg mice (Supplementary Fig. 4B, C). In ELISA, rifampicin significantly reduced the levels of A β 40 and A β 42 in the

TBS-soluble fraction and tended to decrease them in the SDS-soluble fraction, but showed no discernible effect in the FA-soluble fraction (Fig. 4C, D). A β oligomers were reduced in the TBS- and SDS-soluble fractions and were undetectable in the FA-soluble fraction in both commercially available sandwich ELISA (Fig. 4E) and homemade direct ELISA with 11A1 antibody (Fig. 4F).

We also examined tau hyperphosphorylation, synapse loss, and microglial activation by staining brain sections with PHF-1 (anti-pSer396/404-tau), anti-synaptophysin, and anti-Iba-1 antibodies, respectively. Rifampicin successfully lowered PHF-1-positive staining in the hippocampal mossy fibers (Supplementary Fig. 5D, E), restored synaptophysin levels in the hippocampal CA3 region (Supplementary Fig. 5F, G), and inhibited microglial activation in the hippocampal CA3 region in a dose-dependent fashion (Supplementary Fig. 5H, I). Rifampicin-mediated recovery of synaptophysin levels was confirmed by Western blot with hippocampal homogenates (Supplementary Fig. 5J, K).

We previously showed that APP_{OSK} mice suffered mitochondrial damage and apoptosis concomitantly with an intraneuronal accumulation of A β oligomers (Nishitsuji et al., 2009; Umeda et al., 2011). Thus, we examined whether rifampicin prevents A β -induced cytochrome c release from the mitochondria and caspase-3 activation, a measure of apoptosis, with mouse hippocampal homogenates. Rifampicin significantly reduced the levels of cytosolic cytochrome c (Supplementary Fig. 6A, B) and caspase-3 activation in Tg mice to levels similar to or lower than those in CMC-treated non-Tg littermates (Supplementary Fig. 6C, D). Thus, oral rifampicin was shown to improve the memory and amyloid pathology in A β oligomer model mice by reducing A β oligomers.

Effects of rifampicin on A β oligomers and amyloid deposition in Tg2576 mice

Based on the above results, we next investigated the effects of rifampicin on wild-type A β -induced amyloid pathology. Tg2576 mice are a well-known mouse model of Alzheimer's disease that produce abundant wild-type A β and starts amyloid deposition from 9-10 months of age (Hsiao et al., 1996). Rifampicin was orally administered to 13-month-old Tg2576 mice (mean body weight 29.5 g) at 0.5 mg/shot every day for 1 month. Brain sections were prepared from 14-month-old rifampicin-treated mice and stained with β 001 antibody for amyloid deposition and 11A1 antibody for A β oligomer accumulation. Rifampicin significantly reduced 11A1-positive staining in the cerebral cortex and hippocampus, but did not clear β 001-positive staining; rather, it appeared to slightly increase amyloid deposition (Fig. 5A, B). Interestingly, A β oligomers were stained in the central area of amyloid plaques (Fig. 5A, and Supplementary Fig. 7A). Brain homogenates and the TBS, SDS, and FA extracts were prepared and subjected to Western blot and ELISA, respectively. Rifampicin did not affect the expression levels of total and human APP (Supplementary Fig. 7B, C). The levels of A β 40 and A β 42 were reduced in the TBS- and SDS-soluble fractions (Fig. 5C, D). In contrast, those in the FA-soluble fraction were increased. This result seems to be consistent with the immunohistochemical observation that rifampicin slightly increased amyloid deposition (Fig. 5A, B). A β oligomers were reduced in the TBS- and SDS-soluble fractions and undetected in the FA-soluble fraction in sandwich ELISA (Fig. 5E), whereas a significant reduction of A β oligomers was observed in all fractions in direct ELISA (Fig. 5F).

We also examined tau hyperphosphorylation, synapse loss, and microglial activation. PHF-1-positive staining in the hippocampal mossy fibers and in the dystrophic neurites around plaques was significantly decreased by rifampicin (Supplementary Fig. 7A, D, E). Rifampicin also prevented the accumulation of Iba-1-positive microglia around plaques (Supplementary Fig. 7A) and restored synaptophysin levels in the hippocampal mossy fibers (Supplementary Fig. 7F, G). The latter finding was confirmed by Western blot with hippocampal homogenates (Supplementary Fig. 7H, I). Thus, oral rifampicin was shown to improve amyloid pathology in standard Alzheimer's disease model mice by reducing A β oligomers but not amyloid deposition.

Effects of rifampicin on memory and tau oligomers in tau609 mice

Tau609 mice are a transgenic mouse model of tauopathy that were designed to express both 3-repeat and 4-repeat human tau (Umeda et al., 2013). Furthermore, they come to dominantly express 4-repeat human tau at adult age by the presence of FTDP-17-related tau intron mutation. This imbalanced expression of tau isoforms leads to tau hyperphosphorylation, tau oligomer formation, synapse loss, and memory impairment at 6 months, microglial activation at 12 months, and neurofibrillary tangle formation and neuronal loss at 15 months (Umeda et al., 2013, 2015). Rifampicin was orally administered to 7-8-month-old tau609 mice (mean body weight 33.5 g) at 0.5 mg/shot every day for 1 month. Compared with age-matched non-Tg littermates, CMC-treated Tg mice showed significantly impaired memory, whereas rifampicin-treated Tg mice exhibited a significant improvement of memory to a similar level (Fig. 6A, B). We repeated the experiment using older tau609 mice. Rifampicin was administered to

14-15-month-old tau609 mice (mean body weight 36.7 g) at 0.5 and 1 mg/shot every day for 1 month. Again, rifampicin recovered the memory of Tg mice in a dose-dependent fashion: at 1 mg/shot, rifampicin improved the memory almost completely (Fig. 6C, D), whereas 0.5 mg/shot of rifampicin showed a significant but not complete, recovery of memory (Fig. 6E, F).

Brain sections were prepared from 15-16-month-old rifampicin-treated mice and stained with tau oligomer-specific T22 antibody. Rifampicin significantly reduced T22-positive staining in hippocampal CA3 regions in a dose-dependent fashion (Fig. 7A, B, and Supplementary Fig. 8A). Brain homogenates were prepared from 15-16-month-old rifampicin-treated mice (at 1 mg/day) and separated into TBS-, sarkosyl-, and GuHCl-soluble fractions. Western blot with brain homogenates revealed no significant differences in the levels of total (pool 2-positive) and human tau (Tau12-positive) between CMC- and rifampicin-treated Tg mice (Supplementary Fig. 8B, C). In direct ELISA with T22 antibody, rifampicin reduced the levels of tau oligomers significantly in the TBS- and sarkosyl-soluble fractions but not in the GuHCl-soluble fraction (Fig. 7C).

Tau hyperphosphorylation was examined with PHF-1, AT8 (anti-pSer202/Thr204-tau), and Ta1505 (anti-pSer413-tau) antibodies. Rifampicin significantly reduced PHF-1-, AT8-, and Ta1505-positive staining in hippocampal mossy fibers in a dose-dependent fashion (Fig. 8A-D, and Supplementary Fig. 8A). In ELISA, no significant differences in the levels of human tau between CMC- and rifampicin-treated Tg mice were detected in all brain fractions (Fig. 8E). Rifampicin reduced the levels of pSer396-tau and pSer199-tau in the TBS- and GuHCl-soluble fractions, but not in the sarkosyl-soluble fraction (Fig. 8F, G).

We also examined the effects of rifampicin on synapse loss and microglial activation. Rifampicin restored synaptophysin levels ([Supplementary Fig. 8D, E](#)) and inhibited microglial activation in the hippocampal CA3 region in a dose-dependent fashion ([Supplementary Fig. 8F, G](#)). Rifampicin-mediated recovery of synaptophysin levels was confirmed by Western blot with hippocampal homogenates ([Supplementary Fig. 8H, I](#)).

Recent studies have suggested that intracellular tau aggregates are cleared, at least in part, by p62-dependent selective autophagy ([Congdon et al., 2012](#); [Schaeffer et al., 2012](#); [Shimada et al., 2012](#); [Ozcelik et al., 2013](#)). p62, also known as sequestosome-1 (SQSTM1), is a ubiquitin- and LC3 (microtubule-associated protein light chain 3)-interacting protein ([Komatsu and Ichimura, 2010](#)). It binds to polyubiquitinated proteins and the resultant p62/protein complex is selectively sequestered in autophagosomes through the interaction between p62 and LC3. Because p62 is constantly degraded by the autophagy-lysosome system, ablation of autophagy leads to marked accumulation of p62, resulting in the formation of p62-positive inclusions ([Komatsu and Ichimura, 2010](#)). Thus, we examined the conversion of LC3-I to LC3-II, a marker of autophagy activation, and the level of p62 in 15-16-month-old rifampicin-treated mice (at 1 mg/day). Compared with non-Tg littermates, CMC-treated tau609 mice showed increased levels of LC3 conversion and p62 ([Supplementary Fig. 9](#)), implying that autophagy was activated in these mice but its function was impaired. Rifampicin significantly reduced the levels of p62 in Tg mice without affecting LC3 conversion, suggesting that rifampicin helps the restoration of autophagy-lysosomal function.

To investigate whether rifampicin directly influences the autophagy-lysosomal function or restores it by reducing intracellular tau oligomers, we examined the levels of LC3 conversion and p62 in cultured cells. Rifampicin treatment at 100 μ M for 2 days resulted in a slight but significant reduction in LC3 conversion (i.e. suppression of autophagy) with no changes in p62 levels in IMR-32 cells ([Supplementary Fig. 10A-D](#)) and no significant changes in either LC3 conversion or p62 in COS-7 cells ([Supplementary Fig. 10E-H](#)). These results indicate that rifampicin does not directly activate autophagy but restores its function by preventing abnormal protein accumulation beyond the capacity of the protein-degrading system. Thus, oral rifampicin was shown to improve the memory and tau pathology in tauopathy model mice by reducing tau oligomers.

Discussion

Rifampicin is a well-known orally available antibiotic used in the treatment of mycobacterium infections, including tuberculosis and leprosy. Rifampicin is lipid-soluble, and following oral administration it is rapidly absorbed and highly distributed throughout the body tissues and body fluids, including the cerebrospinal fluid ([No authors, 2008](#)). Rifampicin can penetrate into cells by passing through the cell membranes as well as into the brain by crossing the blood-brain barrier (BBB). These pharmacokinetic properties make rifampicin a suitable medicine to treat neurodegenerative diseases that show extracellular and intracellular protein aggregates in the CNS.

An epidemiological study revealed that a treated group of patients with leprosy in Japan had a significantly lower incidence of dementia compared with an untreated group (McGeer et al., 1992). Subsequent histological analyses indicated that non-demented leprosy patients aged over 70 years in Japan showed significantly lower levels of senile plaques in the brain than age-matched non-demented non-leprosy subjects (Namba et al., 1992; Chui et al., 1994). These observations led us to speculate that certain medicine(s) prescribed to these patients may have anti-A β activities. Since rifampicin was always used in combination with dapsone and/or clofazimine in the aforementioned treatment of leprosy, we examined rifampicin and dapsone for effects on A β aggregation and toxicity in vitro, finding that rifampicin has inhibitory activities against A β fibrillization and toxicity (Tomiyama et al., 1994, 1996). Following our studies, researchers examined the action of rifampicin against other amyloidogenic proteins, such as α -synuclein. Rifampicin was found to inhibit α -synuclein fibrillization in vitro (Li et al., 2004) and oligomerization within the cultured cells (Xu et al., 2007). When administered intraperitoneally at 25 mg/kg for 3 months, rifampicin decreased α -synuclein accumulation and the associated neurodegeneration in a mouse model of multiple system atrophy (Ubhi et al., 2008). In the present study, we showed that rifampicin inhibited the oligomerization of A β , tau, and α -synuclein in vitro, and when orally administered for 1 month, it attenuated amyloid and tau pathologies and improved memory in mouse models of Alzheimer's disease and tauopathy. These studies collectively indicate that rifampicin has a broad spectrum and can be used for various neurodegenerative diseases alone. On the other hand, recent clinical trial studies have shown that rifampicin failed to prevent disease progression in patients with mild to moderate Alzheimer's disease (Molloy et al., 2013) and possible or probable multiple

system atrophy (Low et al., 2014). These reports support the notion that treatments after disease onset have little effect and emphasize the importance of prevention in neurodegenerative diseases. Sperling et al. (2011) have proposed three stages for the prevention of Alzheimer's disease: primary (before amyloid deposition), secondary (before the onset of mild cognitive impairment), and tertiary prevention (before the onset of dementia). Here we showed that rifampicin is a good candidate for preventive medicine to be used in the secondary and tertiary prevention of Alzheimer's disease. Therefore, we suggest that rifampicin be evaluated at the early presymptomatic stage of neurodegenerative diseases in further studies.

Several mechanisms underlying the preventive actions of rifampicin are presumed. The primary effect of rifampicin is the inhibition of protein oligomerization. Protein oligomers are in a rapid equilibrium with monomers and higher-order assemblies, and the aggregation process of amyloidogenic proteins is thought to take the following pathway: monomers → low-n oligomers → high-molecular-weight oligomers → protofibrils → fibrils. Once fibrils are formed, monomers may come to directly participate in fibril growth. Our results suggest that rifampicin specifically binds to low-n oligomers of amyloidogenic proteins by recognizing a certain conformation that is not formed in physiological oligomers of non-amyloidogenic proteins, to dissociate them into monomers. Inhibition of extracellular A β oligomerization would result in reduced amyloid plaque formation, as seen in a treated group of Japanese leprosy patients (Namba et al., 1992; Chui et al., 1994). Meanwhile, in the present study, rifampicin failed to decrease amyloid deposition in aged Tg2576 mice, despite it evidently clearing A β oligomers in the plaques. This result suggests that rifampicin does not affect preformed fibrils in amyloid plaques and rather promotes their growth by

providing A β monomers to the fibrils. Recent evidence suggests that amyloid plaques are formed to sequester toxic A β oligomers and plaque itself is not toxic (Cheng et al., 2007; Shankar et al., 2008). Rifampicin may mediate the conversion of plaque A β from toxic oligomers to nontoxic fibrils via monomers.

By binding to oligomers, rifampicin would prevent a possible oligomer-membrane interaction. One of the toxic mechanisms of amyloid oligomers is the disruption of membrane impermeability, probably by forming amyloid pores in the membranes (Demuro et al., 2005; Quist et al., 2005). The oligomer-induced membrane damage allows an excess influx of Ca²⁺ into the cells, which causes mitochondrial dysfunction and subsequent reactive oxygen species (ROS) generation in the mitochondria (Mancuso et al., 2006; De Moura et al., 2010). We and others have shown that rifampicin can block the interaction of oligomers/aggregates of islet amyloid polypeptide (also known as amylin) with the cell membranes (Tomiyama et al., 1996; Harroun et al., 2001; Balali-Mood et al., 2005). Even if neurotoxic oligomers happen to attack cells, rifampicin can act as a hydroxyl radical scavenger with its naphthohydroquinone structure (Tomiyama et al., 1996). Free radical generation and the related oxidative stress have been implicated in the mitochondrial damage and cell death of many neurodegenerative diseases (Mancuso et al., 2006; De Felice et al., 2007; De Moura et al., 2010; Nomura et al., 2013). In the present study, rifampicin attenuated the mitochondrial damage and apoptosis in APP_{OSK} mice. This protective effect of rifampicin may be achieved by scavenging ROS as well as by inhibiting A β oligomerization and/or the oligomer-membrane interaction. Our results also indicate that the inhibition of intracellular protein oligomerization leads to the restoration of autophagy-lysosomal function. The autophagy-lysosome pathway, together with the

ubiquitin-proteasome system, participates in the clearance of cytoplasmic abnormal proteins, and its impairment has been suggested in many neurodegenerative diseases (Ghavami et al., 2014; Vidal et al., 2014). Finally, rifampicin may promote the efflux of amyloidogenic proteins from the brain into the periphery. Rifampicin has been shown to facilitate A β clearance by upregulating the expression of low density lipoprotein receptor-related protein-1 and P-glycoprotein at the BBB (Qosa et al., 2012), and such clearance may be more efficient for protein monomers than for oligomers. These mechanisms may synergistically work to protect neurons from toxic oligomers and represent the multifunctional property of rifampicin.

The primary adverse effect of rifampicin is hepatotoxicity (No authors, 2008). In many cases, the liver damage is cured by discontinuing the medication. If necessary, the medication can be resumed after liver function is restored. Meanwhile, rifampicin has been reported to have cytoprotective effects in the brain (Bi et al., 2013). We observed that rifampicin treatment resulted in a suppression of microglial activation in three different model mice. Another problem of rifampicin is its drug-drug interactions. Rifampicin activates the nuclear pregnane X receptor in hepatocytes that in turn upregulates the expression of cytochrome P450 enzymes and P-glycoprotein: the former metabolizes many drugs and the latter mediates drug adsorption and efflux (Chen and Raymond, 2006). The rifampicin-induced alteration of drug metabolism leads to a decreased efficacy of drugs concomitantly administered with rifampicin. These adverse effects of rifampicin may cause serious problems when used for a long period. However, it is noteworthy that in the present study, only 1-month treatment of rifampicin demonstrated potent effects against oligomers. Similar effects may be achieved at lower doses if rifampicin treatment is continued for longer periods of time. In addition, our

data indicate that the dose of rifampicin necessary for cognitive improvement was lower in younger mice than in older mice. This observation suggests that if rifampicin treatment is started at the early presymptomatic stage of the disease, the dose of rifampicin can be reduced to levels in which any adverse effects of rifampicin are minimized. Although our results indicate that rifampicin binds to only amyloidogenic protein oligomers, we cannot exclude the possibility that rifampicin interacts with physiological oligomes with the β -sheet structure to disturb their function. To avoid such undesired interaction and for developing more specific, safer preventive medicine, further studies are necessary on the interaction between rifampicin and protein oligomers.

To concluded, our results indicate that rifampicin has the properties required for preventive medicines against neurodegenerative diseases: i.e. orally available, little adverse effects, and good efficacy at reducing extracellular and intracellular neurotoxic oligomers with a broad spectrum. Thus, rifampicin could be a promising, ready-to-use medicine for the prevention of Alzheimer's disease and other neurodegenerative diseases.

Acknowledgments

We thank Taro Nishiyama, Saya Tanaka, Naomi Sakama, Reina Fujita, and Maiko Mori for technical assistance, and Peter Karagiannis for reading the manuscript.

Funding

This study was supported by the Grants-in-Aid for Scientific Research from the Ministry of Education, Culture, Sports, Science and Technology of Japan (no. 23110514, 24659434, 25290018); by the Grants-in-Aid from the Ministry of Health, Labour, and Welfare, Japan; and in part by the Strategic Research Program for Brain Sciences (CREST), the Ministry of Education, Culture, Sports, Science and Technology of Japan.

Supplementary material

Supplementary material is available at *Brain* online.

References

- Balali-Mood K, Ashley RH, Hauss T, Bradshaw JP. Neutron diffraction reveals sequence-specific membrane insertion of pre-fibrillar islet amyloid polypeptide and inhibition by rifampicin. *FEBS Lett* 2005;579:1143-1148.
- Bastianetto S, Yao ZX, Papadopoulos V, Quirion R. Neuroprotective effects of green and black teas and their catechin gallate esters against β -amyloid-induced toxicity. *Eur J Neurosci* 2006;23:55-64.
- Bi W, Zhu L, Jing X, Tao E. Rifampicin and Parkinson's disease. *Neurol Sci* 2013;34:137-141.
- Castillo-Carranza DL, Guerrero-Muñoz MJ, Sengupta U, Hernandez C, Barrett AD, Dineley K, et al. Tau immunotherapy modulates both pathological tau and upstream amyloid pathology in an Alzheimer's disease mouse model. *J Neurosci* 2015;35:4857-4868.
- Chen J, Raymond K. Roles of rifampicin in drug-drug interactions: underlying molecular mechanisms involving the nuclear pregnane X receptor. *Ann Clin Microbiol Antimicrob* 2006;5:3.

- Cheng IH, Scearce-Levie K, Legleiter J, Palop JJ, Gerstein H, Bien-Ly N, et al.
Accelerating amyloid-beta fibrillization reduces oligomer levels and functional deficits in Alzheimer disease mouse models. *J Biol Chem* 2007;282:23818-23828.
- Chui DH, Tabira T, Izumi S, Koya G, Ogata J. Decreased β -amyloid and increased abnormal Tau deposition in the brain of aged patients with leprosy. *Am J Pathol* 1994;145:771-775.
- Cleary JP, Walsh DM, Hofmeister JJ, Shankar GM, Kuskowski MA, Selkoe DJ, et al.
Natural oligomers of the amyloid- β protein specifically disrupt cognitive function. *Nat Neurosci* 2005;8:79-84.
- Clinton LK, Blurton-Jones M, Myczek K, Trojanowski JQ, LaFerlaet FM. Synergistic Interactions between A β , tau, and α -synuclein: acceleration of neuropathology and cognitive decline. *J Neurosci* 2010;30:7281-7289.
- Congdon EE, Wu JW, Myeku N, Figueroa YH, Herman M, Marinec PS, et al.
Methylthioninium chloride (methylene blue) induces autophagy and attenuates tauopathy in vitro and in vivo. *Autophagy* 2012;8:609-622.
- Danzer KM, Krebs SK, Wolff M, Birk G, Hengerer B. Seeding induced by α -synuclein oligomers provides evidence for spreading of α -synuclein pathology. *J Neurochem* 2009;111:192-203.
- De Felice FG, Velasco PT, Lambert MP, Viola K, Fernandez SJ, Ferreira ST, et al. A β oligomers induce neuronal oxidative stress through an N-methyl-D-aspartate receptor-dependent mechanism that is blocked by the Alzheimer drug memantine. *J Biol Chem* 2007;282:11590-11601.
- De Moura MB, Dos Santos LS, Van Houten B. Mitochondrial dysfunction in neurodegenerative diseases and cancer. *Environ Mol Mutagen* 2010;51:391-405.

- Demuro A, Mina E, Kaye R, Milton SC, Parker I, Glabe CG. Calcium dysregulation and membrane disruption as a ubiquitous neurotoxic mechanism of soluble amyloid oligomers. *J Biol Chem* 2005;280:17294-17300.
- Diógenes MJ, Dias RB, Rombo DM, Vicente Miranda H, Maiolino F, Guerreiro P, et al. Extracellular α -synuclein oligomers modulate synaptic transmission and impair LTP via NMDA-receptor activation. *J Neurosci* 2012;32:11750-11762.
- Galvin JE, Lee VM, Trojanowski JQ. Synucleinopathies: clinical and pathological implications. *Arch Neurol* 2001;58:186-190.
- Ghavami S, Shojaei S, Yeganeh B, Ande SR, Jangamreddy JR, Mehrpour M, et al. Autophagy and apoptosis dysfunction in neurodegenerative disorders. *Prog Neurobiol* 2014;112:24-49.
- Hamaguchi T, Ono K, Murase A, Yamada M. Phenolic compounds prevent Alzheimer's pathology through different effects on the amyloid- β aggregation pathway. *Am J Pathol* 2009;175:2557-2565.
- Harroun TA, Bradshaw JP, Ashley RH. Inhibitors can arrest the membrane activity of human islet amyloid polypeptide independently of amyloid formation. *FEBS Lett* 2001;507:200-204.
- Imbimbo BP, Giardina GA. γ -Secretase inhibitors and modulators for the treatment of Alzheimer's disease: disappointments and hopes. *Curr Top Med Chem* 2011;11:1555-1570.
- Komatsu M, Ichimura Y. Physiological significance of selective degradation of p62 by autophagy. *FEBS Lett* 2010;584:1374-1378.
- Kondo T, Asai M, Tsukita K, Kutoku Y, Ohsawa Y, Sunada Y, et al. Modeling Alzheimer's disease with iPSCs reveals stress phenotypes associated with

- intracellular A β and differential drug responsiveness. *Cell Stem Cell* 2013;12:487-496.
- Lambert MP, Barlow AK, Chromy BA, Edwards C, Freed R, Liosatos M, et al. Diffusible, nonfibrillar ligands derived from A β 1-42 are potent central nervous system neurotoxins. *Proc Natl Acad Sci USA* 1998;95:6448-6453.
- Lambert MP, Velasco PT, Chang L, Viola KL, Fernandez S, Lacor PN, et al. Monoclonal antibodies that target pathological assemblies of A β . *J Neurochem* 2007;100:23-35.
- Langer F, Eisele YS, Fritschi SK, Staufenbiel M, Walker LC, Juckeret M. Soluble A β seeds are potent inducers of cerebral β -amyloid deposition. *J Neurosci* 2011;31:14488-14495.
- Larson ME, Sherman MA, Greimel S, Kuskowski M, Schneider JA, Bennett DA, et al. Soluble α -synuclein is a novel modulator of Alzheimer's disease pathophysiology. *J Neurosci* 2012;32:10253-10266.
- Lasagna-Reeves CA, Castillo-Carranza DL, Sengupta U, Guerrero-Munoz MJ, Kiritoshi T, Neugebauer V, et al. Alzheimer brain-derived tau oligomers propagate pathology from endogenous tau. *Sci Rep* 2012;2:700.
- Lee VM, Goedert M, Trojanowski JQ. Neurodegenerative tauopathies. *Annu Rev Neurosci* 2001;24:1121-1159.
- Li J, Zhu M, Rajamani S, Uversky VN, Fink AL. Rifampicin inhibits α -synuclein fibrillation and disaggregates fibrils. *Chem Biol* 2004;11:1513-1521.
- Lim GP, Chu T, Yang F, Beech W, Frautschy SA, Cole GM. The curry spice curcumin reduces oxidative damage and amyloid pathology in an Alzheimer transgenic mouse. *J Neurosci* 2001;21:8370-8377.

- Low PA, Robertson D, Gilman S, Kaufmann H, Singer W, Biaggioni I, et al. Efficacy and safety of rifampicin for multiple system atrophy: a randomised, double-blind, placebo-controlled trial. *Lancet Neurol* 2014;13:268-275.
- Mancuso M, Coppede F, Migliore L, Siciliano G, Murri L. Mitochondrial dysfunction, oxidative stress and neurodegeneration. *J Alzheimers Dis* 2006;10:59-73.
- Martin ZS, Neugebauer V, Dineley KT, Kaye R, Zhang W, Reese LC, et al. α -Synuclein oligomers oppose long-term potentiation and impair memory through a calcineurin-dependent mechanism: relevance to human synucleopathic diseases. *J Neurochem* 2012;120:440-452.
- McGeer PL, Harada N, Kimura H, McGeer EG, Schulzer M. Prevalence of dementia amongst elderly Japanese with leprosy: apparent effect of chronic drug therapy. *Dementia* 1992;3:146-149.
- McLaurin J, Golomb R, Jurewicz A, Antel JP, Fraser PE. Inositol stereoisomers stabilize an oligomeric aggregate of Alzheimer amyloid β peptide and inhibit $A\beta$ -induced toxicity. *J Biol Chem* 2000;275:18495-18502.
- McLaurin J, Kierstead ME, Brown ME, Hawkes CA, Lambermon MH, Phinney AL, et al. Cyclohexanehexol inhibitors of $A\beta$ aggregation prevent and reverse Alzheimer phenotype in a mouse model. *Nat Med* 2006;12:801-808.
- Molloy DW, Standish TI, Zhou Q, Guyatt G, DARAD Study Group. A multicenter, blinded, randomized, factorial controlled trial of doxycycline and rifampin for treatment of Alzheimer's disease: the DARAD trial. *Int J Geriatr Psychiatry* 2013;28:463-470.
- Namba Y, Kawatsu K, Izumi S, Ueki A, Ikeda K. Neurofibrillary tangles and senile plaques in brain of elderly leprosy patients. *Lancet* 1992;340:978.

- Nishitsuji K, Tomiyama T, Ishibashi K, Ito K, Teraoka R, Lambert MP, et al. The E693 Δ mutation in amyloid precursor protein increases intracellular accumulation of amyloid β oligomers and causes endoplasmic reticulum stress-induced apoptosis in cultured cells. *Am J Pathol* 2009;174:957-969.
- No authors. *Rifampin. Tuberculosis (Edinb)* 2008;8:151-154.
- Nomura S, Umeda T, Tomiyama T, Mori H. The E693 Δ (Osaka) mutation in amyloid precursor protein potentiates cholesterol-mediated intracellular amyloid β toxicity via its impaired cholesterol efflux. *J Neurosci Res* 2013;91:1541-1550.
- Ono K, Yoshiike Y, Takashima A, Hasegawa K, Naiki H, Yamada M. Potent anti-amyloidogenic and fibril-destabilizing effects of polyphenols in vitro: implications for the prevention and therapeutics of Alzheimer's disease. *J Neurochem* 2003;87:172-181.
- Ono K, Hasegawa K, Naiki H, Yamada M. Curcumin has potent anti-amyloidogenic effects for Alzheimer's β -amyloid fibrils in vitro. *J Neurosci Res* 2004;75:742-750.
- Ono K, Condron MM, Teplow DB. Structure-neurotoxicity relationships of amyloid β -protein oligomers. *Proc Natl Acad Sci USA* 2009;106:14745-14750.
- Ono K, Li L, Takamura Y, Yoshiike Y, Zhu L, Han F, et al. Phenolic compounds prevent amyloid β -protein oligomerization and synaptic dysfunction by site-specific binding. *J Biol Chem* 2012;287:14631-14643.
- Ozcelik S, Fraser G, Castets P, Schaeffer V, Skachokova Z, Breu K, et al. Rapamycin attenuates the progression of tau pathology in P301S tau transgenic mice. *PLoS One* 2013;8:e62459.

- Panza F, Logroscino G, Imbimbo BP, Solfrizzi V. Is there still any hope for amyloid-based immunotherapy for Alzheimer's disease? *Curr Opin Psychiatry* 2014;27:128-137.
- Qosa H, Abuznait AH, Hill RA, Kaddoumi A. Enhanced brain amyloid- β clearance by rifampicin and caffeine as a possible protective mechanism against Alzheimer's disease. *J Alzheimers Dis* 2012;31:151-165.
- Quist A, Doudevski I, Lin H, Azimova R, Ng D, Frangione B, et al. Amyloid ion channels: a common structural link for protein-misfolding disease. *Proc Natl Acad Sci USA* 2005;102:10427-10432.
- Rezai-Zadeh K, Arendash GW, Hou H, Fernandez F, Jensen M, Runfeldt M, et al. Green tea epigallocatechin-3-gallate (EGCG) reduces β -amyloid mediated cognitive impairment and modulates tau pathology in Alzheimer transgenic mice. *Brain Res* 2008;1214:177-187.
- Schaeffer V, Lavenir I, Ozcelik S, Tolnay M, Winkler DT, Goedert M. Stimulation of autophagy reduces neurodegeneration in a mouse model of human tauopathy. *Brain* 2012;135:2169-2177.
- Shankar GM, Li S, Mehta TH, Garcia-Munoz A, Shepardson NE, Smith I, et al. Amyloid-beta protein dimers isolated directly from Alzheimer's brains impair synaptic plasticity and memory. *Nat Med* 2008;14:837-842.
- Shimada K, Motoi Y, Ishiguro K, Kambe T, Matsumoto SE, Itaya M, et al. Long-term oral lithium treatment attenuates motor disturbance in tauopathy model mice: implications of autophagy promotion. *Neurobiol Dis* 2012;46:101-108.
- Sperling RA, Jack CR Jr, Aisen PS. Testing the right target and right drug at the right stage. *Sci Transl Med*. 2011;3:111cm33.

- Takahashi R, Ono K, Takamura Y, Mizuguchi M, Ikeda T, Nishijo H, et al. Phenolic compounds prevent the oligomerization of α -synuclein and reduce synaptic toxicity. *J Neurochem* 2015;134:943-955.
- Tomiyama T, Asano S, Suwa Y, Morita T, Kataoka K, Mori H, et al. Rifampicin prevents the aggregation and neurotoxicity of amyloid β protein in vitro. *Biochem Biophys Res Commun* 1994;204:76-83.
- Tomiyama T, Shoji A, Kataoka K, Suwa Y, Asano S, Kaneko H, et al. Inhibition of amyloid β protein aggregation and neurotoxicity by rifampicin. Its possible function as a hydroxyl radical scavenger. *J Biol Chem* 1996;271:6839-6844.
- Tomiyama T, Kaneko H, Kataoka K, Asano S, Endo N. Rifampicin inhibits the toxicity of pre-aggregated amyloid peptides by binding to peptide fibrils and preventing amyloid-cell interaction. *Biochem J* 1997;322:859-865.
- Tomiyama T, Nagata T, Shimada H, Teraoka R, Fukushima A, Kanemitsu H, et al. A new amyloid β variant favoring oligomerization in Alzheimer's-type dementia. *Ann Neurol* 2008;63:377-387.
- Tomiyama T, Matsuyama S, Iso H, Umeda T, Takuma H, Ohnishi K, et al. A mouse model of amyloid β oligomers: their contribution to synaptic alteration, abnormal tau phosphorylation, glial activation, and neuronal loss in vivo. *J Neurosci* 2010;30:4845-4856.
- Ubhi K, Rockenstein E, Mante M, Patrick C, Adame A, Thukral M, et al. Rifampicin reduces α -synuclein in a transgenic mouse model of multiple system atrophy. *Neuroreport* 2008;19:1271-1276.
- Umeda T, Tomiyama T, Sakama N, Tanaka S, Lambert MP, Klein WL, et al. Intraneuronal amyloid β oligomers cause cell death via endoplasmic reticulum

- stress, endosomal/lysosomal leakage, and mitochondrial dysfunction in vivo. *J Neurosci Res* 2011;89:1031-1042.
- Umeda T, Yamashita T, Kimura T, Ohnishi K, Takuma H, Ozeki T, et al. Neurodegenerative disorder FTDP-17-related tau intron 10 +16C → T mutation increases tau exon 10 splicing and causes tauopathy in transgenic mice. *Am J Pathol* 2013;183:211-225.
- Umeda T, Maekawa S, Kimura K, Takashima A, Tomiyama T, Mori H. Neurofibrillary tangle formation by introducing wild-type human tau into APP transgenic mice. *Acta Neuropathol* 2014;127:685-698.
- Umeda T, Eguchi H, Kunori Y, Matsumoto Y, Taniguchi T, Mori H, et al. Passive immunotherapy of tauopathy targeting pSer413-tau: a pilot study in mice. *Ann Clin Transl Neurol* 2015;2:241-255.
- Vidal RL, Matus S, Bargsted L, Hetz C. Targeting autophagy in neurodegenerative diseases. *Trends Pharmacol Sci* 2014;35:583-591.
- von Bergen M, Barghorn S, Biernat J, Mandelkow EM, Mandelkow E. Tau aggregation is driven by a transition from random coil to beta sheet structure. *Biochim Biophys Acta* 2005;1739:158-166.
- Walsh DM, Klyubin I, Fadeeva JV, Cullen WK, Anwyl R, Wolfe MS, et al. Naturally secreted oligomers of amyloid β protein potently inhibit hippocampal long-term potentiation in vivo. *Nature* 2002;416:535-539.
- Xu J, Wei C, Xu C, Bennett MC, Zhang G, Li F, et al. Rifampicin protects PC12 cells against MPP⁺-induced apoptosis and inhibits the expression of an α -Synuclein multimer. *Brain Res* 2007;1139:220-225.

Yang F, Lim GP, Begum AN, Ubeda OJ, Simmons MR, Ambegaokar SS, et al.

Curcumin inhibits formation of amyloid β oligomers and fibrils, binds plaques, and reduces amyloid in vivo. *J Biol Chem* 2005;280:5892-5901.

Figure legends

Figure 1. Effects of candidate compounds on intracellular accumulation of A β oligomers in cultured cells. (A) COS-7 cells transfected with APP_{OSK} were cultured for 2 days in the presence of rifampicin (RFP), curcumin (Cur), myricetin (Myr), EGCG, and scyllo-inositol (Scyllo) at 100 μ M and stained with A β oligomer-selective NU-1 antibody (green) and DAPI (blue) after fixation. Note that the number of cells was decreased due to cell death when the tested compound was not effective against A β oligomer accumulation. Scale bars, 50 μ m in upper panel and 30 μ m in lower panel. (B) NU-1 fluorescence intensity in a constant field of the culture was quantified, and the number of DAPI-positive cells in the same field was counted. Each bar represents the mean fluorescence intensity/cell \pm SEM (n = 3 for all groups). (C) Non-treated and rifampicin-treated cells were harvested and subjected to Western blot with 82E1 antibody for A β , C40 antibody for APP, and antibody for actin. (D) The levels of A β monomers, dimers, and trimers + CTF β (carboxyl terminal fragment β of APP) in cell lysates were quantified. Each bar represents the mean \pm SEM (n = 3 for both groups). (E-G) Conditioned media were collected and subjected to ELISA to measure A β 40 (E), A β 42 (F), and A β oligomers (G). Each bar represents the mean \pm SEM (n = 7 for both groups).

Figure 2. Effects of rifampicin on oligomer formation of A β , tau, and α -synuclein under cell-free conditions. A β 40 (A), A β 42 (B), tau-441 (C), α -synuclein (D), and GST (E) were incubated at 25 μ M with rifampicin (RFP) at 25 μ M (molar ratio of 1:1) or 100 μ M (1:4) and cross-linked by PICUP. The samples were subjected to SDS-PAGE under reducing conditions, and the oligomer formation by each protein was

visualized by silver staining. M, molecular size marker; UnXL, uncross-linked samples; 1x, RFP 25 μ M; 4x, RFP 100 μ M. (F, G) A β 42 peptide with the Osaka mutation was mixed at 25 μ M with rifampicin at 25 μ M or 100 μ M and subjected to direct oligomer ELISA (F) and sandwich A β 42 ELISA (G). Each bar represents the mean \pm SEM (n = 3 for each group).

Figure 3. Effects of rifampicin on the memory of APP_{OSK} mice. (A) Rifampicin dissolved in 0.5% CMC was orally administered to 11-12-month-old APP_{OSK} mice at 0.5 mg/shot every day for 1 month. The spatial reference memory of mice was examined using the Morris water maze, in which mice were trained to swim to the hidden platform for 5 consecutive days. Each point represents the mean latency of five trials per day \pm SEM (n = 10 for Non-Tg; n = 9 for each Tg group). * p = 0.0034 vs. Non-Tg and = 0.0119 vs. RFP. (B) At day 6, retention of memory was assessed by a probe trial for 60 s with the platform removed. Each bar represents the mean time occupancy \pm SEM in the target quadrant. (C) Rifampicin was administered to 17-month-old APP_{OSK} mice at 0.5 and 1 mg/shot every day for 1 month, and the Morris water maze was performed. n = 16 for Non-Tg; n = 10 for each Tg group. ** p < 0.0001 vs. Non-Tg and = 0.0060 vs. 1 mg RFP; * p = 0.0073 vs. Non-Tg. (D) Retention of memory was assessed by a probe trial.

Figure 4. Effects of rifampicin on A β oligomer accumulation in APP_{OSK} mice. (A) Brain sections prepared from 18-month-old rifampicin-treated mice were stained with A β oligomer-specific 11A1 antibody. Photographs were taken from the cerebral cortex

(CTX) and hippocampal CA1 and CA3 regions. Scale bar, 30 μm . **(B)** A β oligomer accumulation was evaluated by quantifying 11A1-staining intensities in each photograph. Each bar represents the mean intensity \pm SEM ($n = 5$ for all groups). **(C-F)** Brain homogenates from 18-month-old rifampicin-treated mice (at 1 mg/day) were separated into TBS-, SDS-, and FA-soluble fractions and diluted 10-, 20-, and 100-fold, respectively. The levels of A β 40 **(C)**, A β 42 **(D)**, and A β oligomers **(E)** in each fraction were measured by ELISA. Each bar represents the mean \pm SEM ($n = 4$ for both groups). The original concentrations of each A β species before sample dilution were calculated and are shown. The levels of A β oligomers were also measured by direct ELISA with 11A1 antibody **(F)**, where each fraction was diluted 2-fold and allowed to coat ELISA plates.

Figure 5. Effects of rifampicin on amyloid deposition and A β oligomer accumulation in Tg2576 mice. **(A)** Brain serial sections prepared from 14-month-old rifampicin-treated mice (at 0.5 mg/day) were stained with β 001 (anti-A β) and 11A1 (anti-A β oligomers) antibodies. Photographs were taken from the cerebrum including the hippocampus at low magnification and from the hippocampus at high magnification. Scale bars, 100 μm . **(B)** Amyloid deposition and A β oligomer accumulation were evaluated by quantifying β 001- and 11A1-staining areas (% of the whole area) in each photograph of the hippocampus. Each bar represents the mean \pm SEM ($n = 4$ for CMC-treated Tg and $n = 6$ for rifampicin-treated Tg). **(C-F)** Brain homogenates were separated into TBS-, SDS-, and FA-soluble fractions and diluted 10-, 20-, and 100-fold, respectively. The levels of A β 40 **(C)**, A β 42 **(D)**, and A β oligomers **(E)** in each fraction were measured by ELISA. Each bar represents the mean \pm SEM ($n = 4$ for both groups).

The original concentrations of each A β species before sample dilution were calculated and are shown. The levels of A β oligomers were also measured by direct ELISA with 11A1 antibody (**F**), where each fraction was diluted 2-fold and allowed to coat ELISA plates.

Figure 6. Effects of rifampicin on the memory of tau609 mice. (**A**) Rifampicin was administered to 7-8-month-old tau609 mice at 0.5 mg/shot every day for 1 month, and the Morris water maze was performed. Each point represents the mean latency of five trials per day \pm SEM (n = 10 for Non-Tg; n = 9 for CMC-treated Tg; and n = 8 for rifampicin-treated Tg). * p = 0.0009 vs. Non-Tg and = 0.0117 vs. RFP. (**C**) Rifampicin was administered to 14-15-month-old tau609 mice at 0.5 mg/shot every day for 1 month, and the Morris water maze was performed. n = 10 for Non-Tg; n = 9 for CMC-treated Tg; and n = 8 for rifampicin-treated Tg. * p < 0.0001 vs. Non-Tg and = 0.0011 vs. RFP. (**E**) Rifampicin was administered to 14-15-month-old tau609 mice at 1 mg/shot every day for 1 month, and the Morris water maze was performed. n = 11 for Non-Tg; n = 7 for each Tg group. * p = 0.0150 vs. Non-Tg. (**B, D, F**) Retention of memory was assessed by a probe trial. Each bar represents the mean time occupancy \pm SEM in the target quadrant.

Figure 7. Effects of rifampicin on tau oligomer accumulation in tau609 mice. (**A**) Brain sections were prepared from 15-16-month-old rifampicin-treated mice and stained with tau oligomer-specific T22 antibody. All photographs were taken from the hippocampal CA3 region. Scale bar, 50 μ m. (**B**) Tau oligomer accumulation was

evaluated by quantifying T22-staining intensities in each photograph. Each bar represents the mean intensity \pm SEM (n = 10 for Non-Tg; n = 10 for CMC-treated Tg; n = 3 for 0.5 mg rifampicin-treated Tg; and n = 6 for 1 mg rifampicin-treated Tg). (C) Brain homogenates from 15-16-month-old rifampicin-treated mice (at 1 mg/day) were separated into TBS-, sarkosyl-, and GuHCl-soluble fractions. The levels of tau oligomers were measured by direct ELISA with T22 antibody, where each fraction was diluted 2-fold and allowed to coat ELISA plates. Each bar represents the mean \pm SEM (n = 3 for CMC-treated Tg and n = 5 for rifampicin-treated Tg).

Figure 8. Effects of rifampicin on tau hyperphosphorylation in tau609 mice. (A)

Brain sections prepared from 15-16-month-old rifampicin-treated mice were stained with PHF-1, AT8, and Ta1505 antibodies. All photographs were taken from the hippocampal CA3 region. Scale bar, 50 μ m. (B-D) Tau phosphorylation was estimated by quantifying PHF-1- (B), AT8- (C), and Ta1505- (D) staining intensities in the hippocampal mossy fiber field. Each bar represents the mean intensity \pm SEM (in PHF-1- and AT8- staining, n = 10 for Non-Tg; n = 10 for CMC-treated Tg; n = 3 for 0.5 mg rifampicin-treated Tg; and n = 6 for 1 mg rifampicin-treated Tg; in Ta1505-staining, n = 5 for Non-Tg; n = 7 for CMC-treated Tg; n = 3 for 0.5 mg rifampicin-treated Tg; and n = 6 for 1 mg rifampicin-treated Tg). (E-G) TBS-, sarkosyl-, and GuHCl-soluble brain fractions prepared from 15-16-month-old rifampicin-treated mice (at 1 mg/day) were diluted 2,000-, 200-, and 200-fold, respectively, for the measurement of total tau (E) and pSer199-tau (G); and 200-, 20-, and 20-fold, respectively, for pSer396-tau (F) by ELISA. Each bar represents the mean \pm SEM (n =

3 for CMC-treated Tg and $n = 5$ for rifampicin-treated Tg). The original concentrations of each tau species before sample dilution were calculated and are shown.

Supplementary material

Materials and methods

Effects of rifampicin on A β production in cultured cells

COS-7 cells were transfected with wild-type APP and C99 (i.e. β -cut fragment of APP) constructs as described previously ([Nishitsuji et al., 2009](#)) and cultured in the presence of 100 μ M rifampicin for 2 days. As a control, DMSO was added to culture medium, which was used as a solvent for rifampicin. Cells were harvested, lysed and subjected to Western blot with C40 antibody for APP and C99, and with anti-actin antibody. Conditioned media were collected and subjected to ELISA to measure the levels of A β 40 and A β 42.

NMR analysis of rifampicin/protein interaction

cDNAs encoding A β 42, tau-441, α -synuclein, and GST with an N-terminal His-tag (MAHHHHHH) were inserted into pOPTH plasmid. These fusion proteins were expressed in *E. coli* BL21 (DE3) grown in M9 minimal medium supplemented with $^{15}\text{NH}_4\text{Cl}$ and ^{13}C -glucose. $^{13}\text{C}/^{15}\text{N}$ -labeled proteins were purified with a Ni-NTA agarose resin (Qiagen, Valencia, CA) followed by gel-filtration, as described previously ([Ono et al., 2012](#); [Takahashi et al., 2015](#)). The purity of the $^{13}\text{C}/^{15}\text{N}$ -labeled proteins was checked by SDS-PAGE and matrix assisted laser desorption/ionization-time of flight mass spectrometry (MALDI-TOF MS). A stock solution of rifampicin (100 mM) was prepared by dissolution in DMSO- d_6 . Aliquots of the rifampicin solution were mixed with the protein solutions into a final concentration of 0.5 mM. The A β 42 samples contained 0.08 mM $^{13}\text{C}/^{15}\text{N}$ -labeled A β 42, 20 mM sodium phosphate (pH 7.4), 50 mM

NaCl, 90 μ M 4,4-dimethyl-4-silapentane-1-sulfonic acid, 90 μ M NaN₃, 0.45% DMSO-d₆, and 10% D₂O; the tau-441 samples contained 0.3 mM ¹³C/¹⁵N-labeled tau-441, 10 mM sodium phosphate (pH 7.4), 50 mM NaCl, 5 mM dithiothreitol, 90 μ M 4,4-dimethyl-4-silapentane-1-sulfonic acid, 90 μ M NaN₃, 0.45% DMSO-d₆, and 10% D₂O; the α -synuclein samples contained 0.045 mM ¹³C/¹⁵N-labeled α -synuclein, 10 mM HEPES (pH 7.4), 50 mM NaCl, 90 μ M 4,4-dimethyl-4-silapentane-1-sulfonic acid, 90 μ M NaN₃, 0.45% DMSO-d₆, and 10% D₂O; and the GST samples contained 0.4 mM ¹³C/¹⁵N-labeled GST, 10 mM sodium phosphate (pH 7.5), 5 mM dithiothreitol, 90 μ M 4,4-dimethyl-4-silapentane-1-sulfonic acid, 90 μ M NaN₃, 0.45% DMSO-d₆, and 10% D₂O. All NMR spectra were obtained with a Bruker Avance 800 MHz spectrometer equipped with a cryoprobe (Bruker BioSpin, Rheinstetten, Germany). NMR data were processed with NMRPipe and analyzed with NMRView, as described previously (Ono et al., 2012; Takahashi et al., 2015).

Thioflavin T assay

A β 42 peptide (Peptide Institute) and GST protein (Sigma-Aldrich) were dissolved to 500 μ M in 60 mM NaOH, sonicated, and diluted to 25 μ M in PBS. The solutions were dispensed into tubes and incubated at 37 °C. Peptide/protein aggregation into the β -sheet conformation was monitored by the thioflavin T assay, as described previously (Tomiyama et al., 1994).

Western blot analysis of mitochondrial damage and apoptosis

COS-7 cells transfected with APP_{OSK} construct were treated with each compound at 1, 10, and 100 μ M. After the 2-day treatment, the cells were harvested, lysed, and

separated into cytosol and mitochondrial fractions using the Cytochrome c Releasing Apoptosis Assay Kit (BioVision, Mountain View, CA), as described previously (Umeda et al., 2011). Samples with equal protein content were subjected to Western blot with anti-cytochrome c antibody (supplied in the kit). Signals were visualized using an LAS-3000 luminescent image analyzer.

Hippocampal tissues from APP_{OSK} mice and non-Tg littermates were homogenized and separated into cytosol and mitochondrial fractions using the Cytochrome c Releasing Apoptosis Assay Kit. The separated fractions with equal protein content were subjected to Western blot with anti-cytochrome c antibody, while the non-separated homogenates with equal protein content were used for Western blot with a mouse monoclonal antibody to cleaved caspase-3 (Cell Signaling Technology, Danvers, MA), as described previously (Umeda et al., 2011).

Western blot analysis of autophagy function

Brain homogenates from tau609 mice and non-Tg littermates with equal protein content were subjected to Western blot with rabbit polyclonal anti-LC3 and anti-p62 antibodies (both from MBL, Nagoya, Japan). Signals were visualized and quantified using an LAS-3000 luminescent image analyzer.

To measure the levels of LC3 conversion and p62 in the homogenates, we first treated IMR-32 cells and COS-7 cells with rifampicin at 100 μ M for 2 days. Cells in a 10-cm dish were then harvested and lysed by sonication in 100 μ l of 1% Triton X-100 in TBS containing 1/100 volumes of protease inhibitor cocktail (P8340). Levels were determined by Western blot, as described above.

Figure legends

Supplementary Figure 1. Effects of rifampicin on A β production in cultured cells.

COS-7 cells transfected with wild-type APP (**A, B**) and C99 (**C, D**) were cultured in the presence and absence of 100 μ M rifampicin for 2 days. (**A, C**) Cells were lysed and subjected to Western blot with C40 antibody for APP and C99. (**B, D**) Conditioned media were subjected to ELISA to measure the levels of A β 40 and A β 42. Each bar represents the mean \pm SEM (n =3 for both groups).

Supplementary Figure 2. Effects of candidate compounds on the toxicity of A β oligomers in cultured cells.

(**A**) COS-7 cells transfected with APP_{OSK} were harvested after the treatment with each compound at 1-100 μ M for 2 days. Mock- and APP_{WT}-transfected cells were also prepared as controls. Cytosol fractions prepared from cell lysates were subjected to Western blot for cytosolic cytochrome c. (**B**) The levels of cytosolic cytochrome c were quantified. Each bar represents the mean \pm SEM (n =3 for all groups except n = 4 for RFP-treated APP_{OSK}) in comparison of mock transfected cells. * p = 0.0008, ** p = 0.0014, *** p = 0.0347, † p = 0.0016, †† p = 0.0053, ‡ p = 0.0081, ‡‡ p = 0.0253, § p = 0.0126, ¶ p = 0.0386 vs. non-treated APP_{OSK}.

Supplementary Figure 3. Binding of rifampicin to A β , tau, and α -synuclein under cell-free conditions.

The interaction of rifampicin with ¹³C/¹⁵N-labeled A β 42 (**A**), tau-441 (**B**), α -synuclein (**C**), and GST (**D**) was analyzed by NMR spectroscopy. ¹H-¹⁵N heteronuclear single quantum coherence (HSQC) spectra of each protein in the absence (**a**) and presence (**b**) of rifampicin, and their overlaid spectra (**c**) are shown. These NMR spectra were taken at 278K (**A**), 283K (**B**), 288K (**C**), and 298K (**D**), respectively.

Supplementary Figure 4. β -Sheet conformation of A β 42 and GST. A β 42 peptide and GST protein at 25 μ M in PBS were incubated at 37 °C. β -Sheet conformation in protein solutions was monitored by the thioflavin T assay. Each point represents the mean \pm SD (n = 4 for both groups).

Supplementary Figure 5. Effects of rifampicin on tau hyperphosphorylation, synapse loss, and microglial activation in APP_{OSK} mice. (A) Images at lower magnification of brain sections stained with 11A1 antibody (see Fig. 4A) are shown. (B) Brain homogenates prepared from 18-month-old rifampicin-treated mice (at 1 mg/day) were subjected to Western blot with C40 antibody for total APP, 6E10 antibody for human APP, and antibody for actin. (C) The levels of total and human APP were quantified, and their ratios to actin were calculated. Each bar represents the mean \pm SEM (n = 4 for all groups). (D-I) Brain sections prepared from 18-month-old rifampicin-treated mice were stained with PHF-1 (D), anti-synaptophysin (F), and anti-Iba-1 (H) antibodies. All photographs were taken from the hippocampal CA3 region. Scale bars, 50 μ m (D), 30 μ m (F), and 50 μ m (H). (E) Tau phosphorylation was estimated by quantifying PHF-1-staining intensities in the hippocampal mossy fiber field. Each bar represents the mean intensity \pm SEM (n = 5 for all groups). (G) Synapse loss was assessed by quantifying synaptophysin fluorescence intensities in the apical dendritic-somata field. Each bar represents the mean intensity \pm SEM (n = 5 for all groups). (I) Microglial activation was evaluated by quantifying Iba-1-staining intensities in each photograph. Each bar represents the mean intensity \pm SEM (n = 5 for Non-Tg; n = 4 for CMC-treated Tg; and n = 5 for each group of rifampicin-treated Tg). (J)

Hippocampal homogenates prepared from 18-month-old rifampicin-treated mice (at 1 mg/day) were subjected to Western blot for synaptophysin. **(K)** The levels of synaptophysin were quantified. Each bar represents the mean \pm SEM (n = 3 for all groups).

Supplementary Figure 6. Effects of rifampicin on mitochondrial damage and apoptosis in APP_{OSK} mice. Hippocampal tissues were dissected from 18-month-old rifampicin-treated mice (at 1 mg/shot). The levels of cytosolic cytochrome c **(A)** and cleaved caspase-3 **(C)** were measured by Western blot. **(B)** Each bar represents the mean level of cytosolic cytochrome c \pm SEM (n = 5 for all groups) in comparison with Non-Tg. **(D)** Each bar represents the mean level of cleaved caspase-3 \pm SEM (n = 4 for all groups) in comparison with Non-Tg.

Supplementary Figure 7. Effects of rifampicin on tau hyperphosphorylation, synapse loss, and microglial activation in Tg2576 mice. **(A)** Brain serial sections prepared from 14-month-old rifampicin-treated mice (at 0.5 mg/day) were stained with β 001 (anti-A β), 11A1 (anti-A β oligomers), PHF-1, and anti-Iba-1 antibodies. Photographs were taken from the cerebral cortex. Scale bar, 30 μ m. **(B)** Brain homogenates prepared from 14-month-old rifampicin-treated mice (at 0.5 mg/day) were subjected to Western blot with C40 antibody for total APP, 6E10 antibody for human APP, and antibody for actin. **(C)** The levels of total and human APP were quantified, and their ratios to actin were calculated. Each bar represents the mean \pm SEM (n = 4 for all groups). **(D)** Brain sections were stained with PHF-1 antibody. Photographs were

taken from the cerebrum including hippocampus. Scale bars, 100 μm . **(E)** Tau phosphorylation was estimated by quantifying PHF-1-staining intensities in the hippocampal mossy fiber field. Each bar represents the mean intensity \pm SEM (n = 4 for CMC-treated Tg and n = 6 for rifampicin-treated Tg). **(F)** Brain sections were stained with anti-synaptophysin antibody. Photographs were taken from the hippocampal CA3 region. Scale bar, 30 μm . **(G)** Synapse loss was assessed by quantifying synaptophysin fluorescence intensities in the apical dendritic-somata field. Each bar represents the mean intensity \pm SEM (n = 5 for Non-Tg; n = 4 for CMC-treated Tg; and n = 6 for rifampicin-treated Tg). **(H)** Hippocampal homogenates were subjected to Western blot for synaptophysin. **(I)** The levels of synaptophysin were quantified. Each bar represents the mean \pm SEM (n = 4 for all groups).

Supplementary Figure 8. Effects of rifampicin on synapse loss and microglial activation in tau609 mice. **(A)** Images at lower magnification of brain sections stained with T22, PHF-1, AT8, and Ta1505 antibodies (see Figs. 7A and 8A) are shown. **(B)** Brain homogenates prepared from 15-16-month-old rifampicin-treated mice (at 1 mg/day) were subjected to Western blot with pool-2 antibody for total tau, Tau12 antibody for human tau, and antibody for actin. Tau mix, mixture of 6 isoforms of human tau; M, molecular size marker. **(C)** The levels of total and human tau were quantified, and their ratios to actin were calculated. Each bar represents the mean \pm SEM (n = 3 for CMC-treated Tg; and n = 5 for rifampicin-treated Tg). **(D-G)** Brain sections prepared from 15-16-month-old rifampicin-treated mice were stained with anti-synaptophysin **(D)** and anti-Iba-1 **(F)** antibodies, respectively. All photographs were taken from the hippocampal CA3 region. Scale bars, 30 μm **(D)** and 50 μm **(F)**.

(E) Synapse loss was assessed by quantifying synaptophysin fluorescence intensities in the apical dendritic-somata field. Each bar represents the mean intensity \pm SEM (n = 10 for Non-Tg; n = 10 for CMC-treated Tg; n = 4 for 0.5 mg rifampicin-treated Tg; and n = 6 for 1 mg rifampicin-treated Tg). (G) Microglial activation was evaluated by quantifying Iba-1-staining intensities in each photograph. Each bar represents mean intensity \pm SEM (n = 10 for Non-Tg; n = 10 for CMC-treated Tg; n = 3 for 0.5 mg rifampicin-treated Tg; and n = 6 for 1 mg rifampicin-treated Tg). (H) Hippocampal homogenates were subjected to Western blot for synaptophysin. (I) The levels of synaptophysin were quantified. Each bar represents the mean \pm SEM (n = 4 for all groups).

Supplementary Figure 9. Effects of rifampicin on autophagy function in tau609

mice. (A) Brain homogenates were prepared from 15-16-month-old rifampicin-treated mice (at 1 mg/shot) and subjected to Western blot with anti-LC3, anti-p62, and anti-actin antibodies. (B-D) The levels of LC3 conversion and p62 were quantified. Each bar represents the mean level of LC3-II \pm SEM (B), the mean ratio of LC3-II/LC3-I \pm SEM (C), and the mean level of p62 \pm SEM (D) (n = 3 for Non-Tg; n = 4 for each Tg group).

Supplementary Figure 10. Effects of rifampicin on autophagy function in cultured

cells. IMR-32 cells (A) and COS-7 cells (E) were treated with rifampicin at 100 μ M for 2 days. The cell lysates were subjected to Western blot with anti-LC3, anti-p62, and anti-actin antibodies. (B-D, F-H) The levels of LC3 conversion and p62 were quantified.

Each bar represents the mean level of LC3-II \pm SEM (**B, F**), the mean ratio of LC3-II/LC3-I \pm SEM (**C, G**), and the mean level of p62 \pm SEM (**D, H**) (n = 3 for all group).

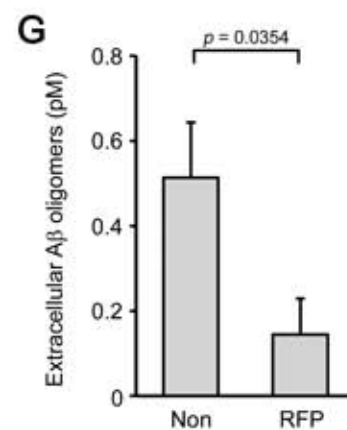
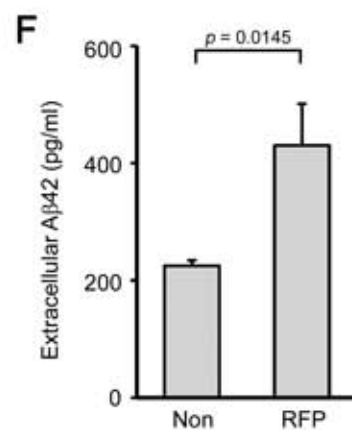
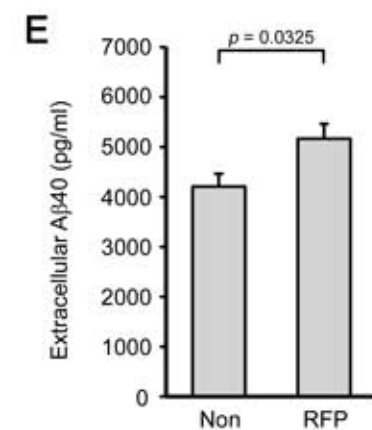
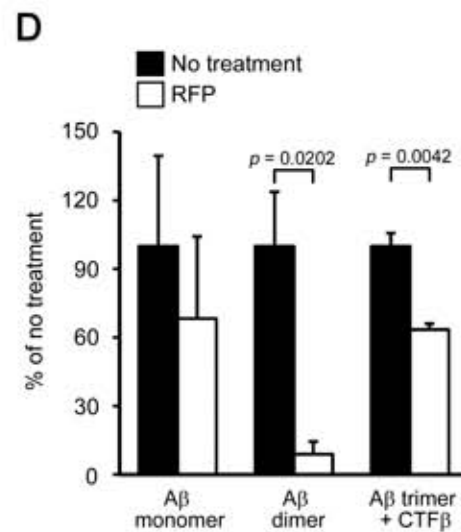
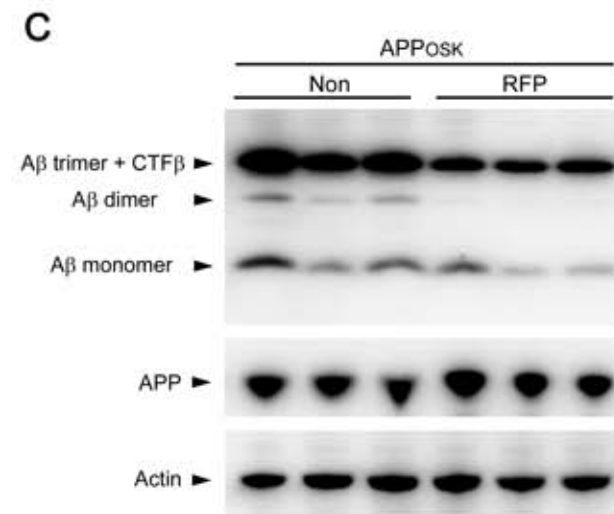
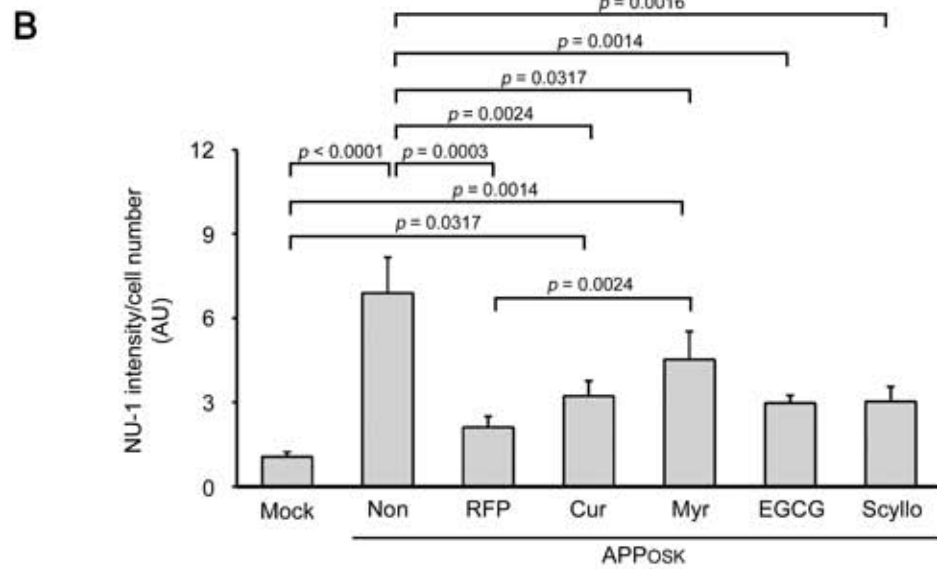
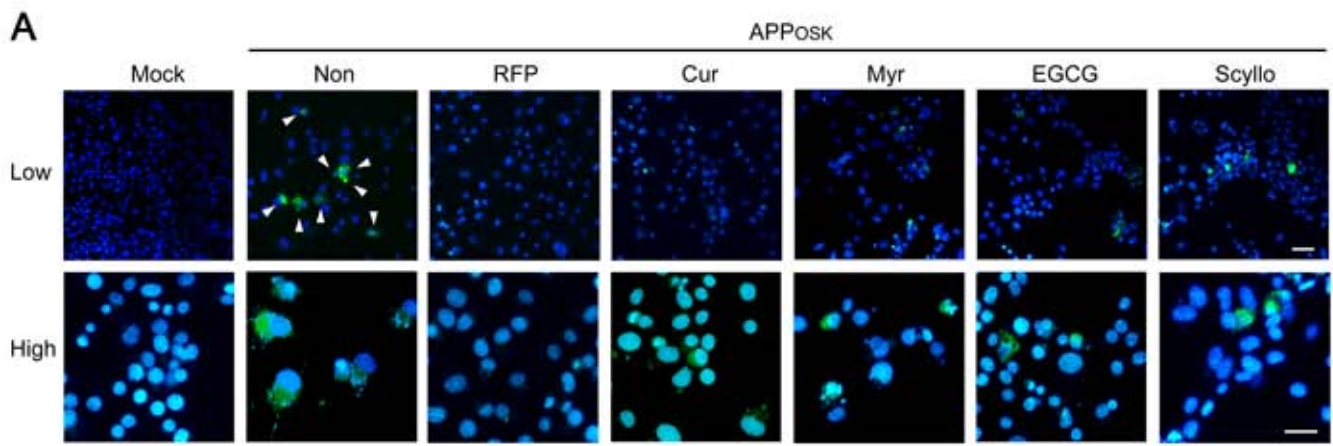


Fig. 1

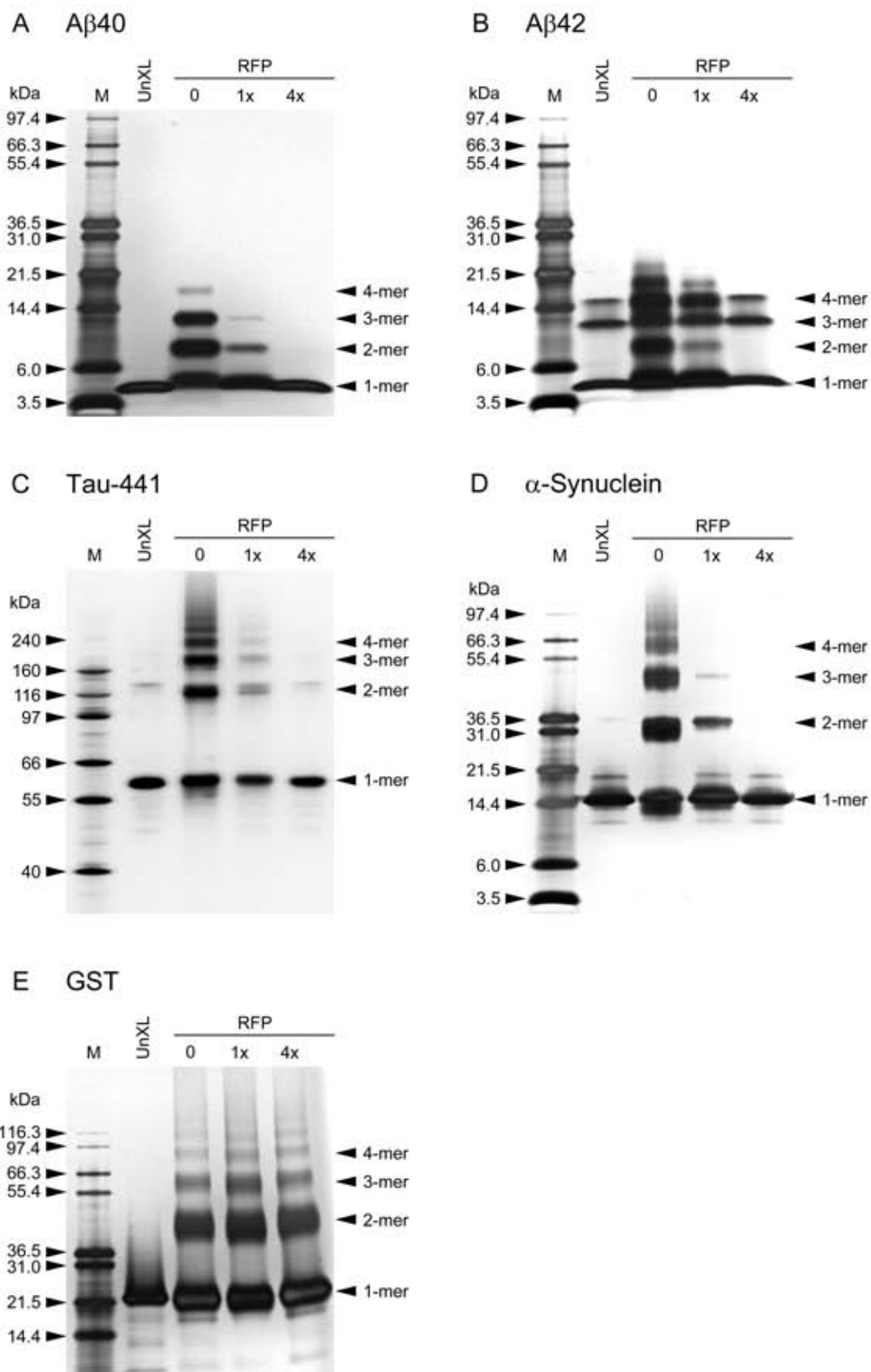


Fig. 2

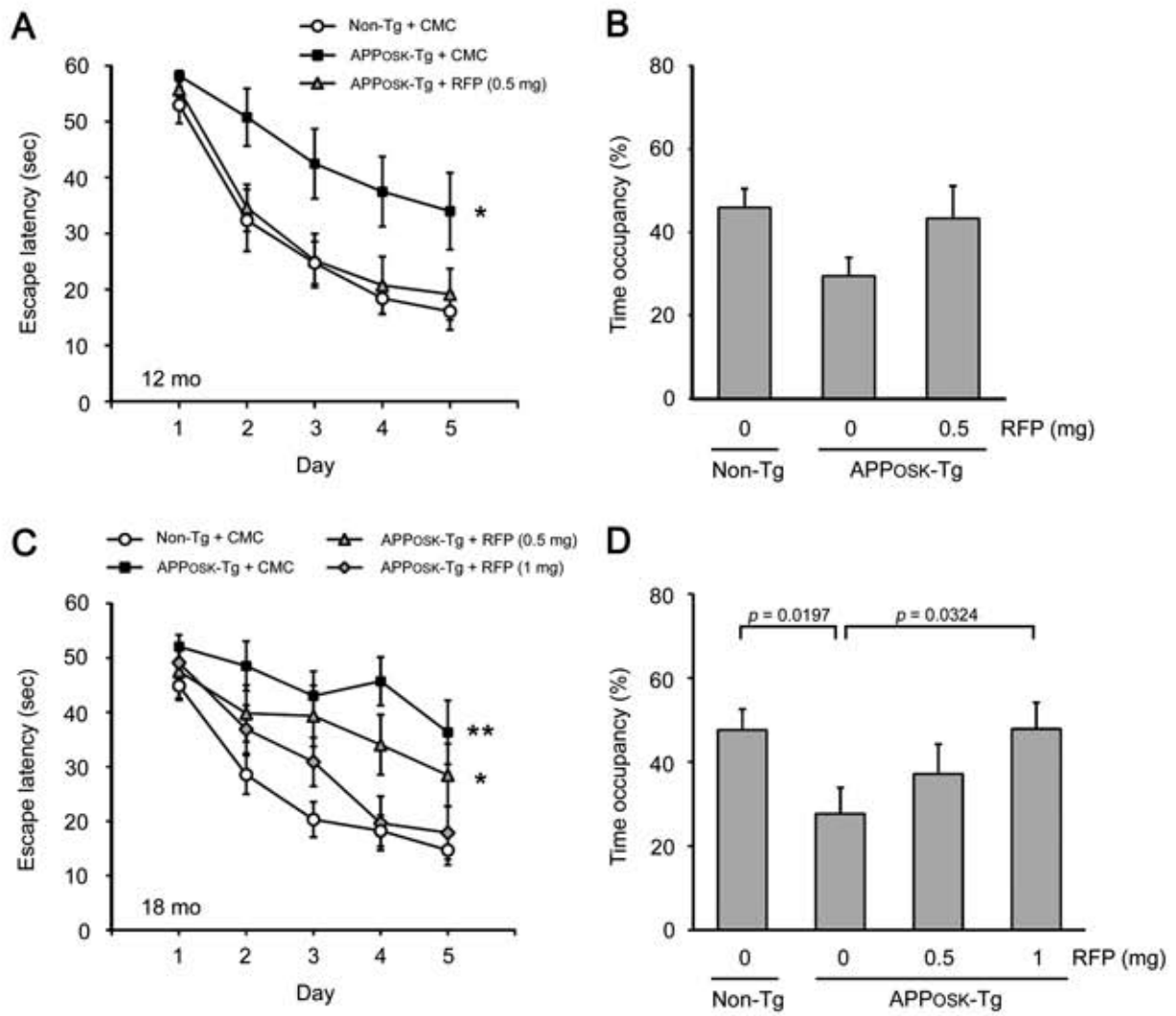


Fig. 3

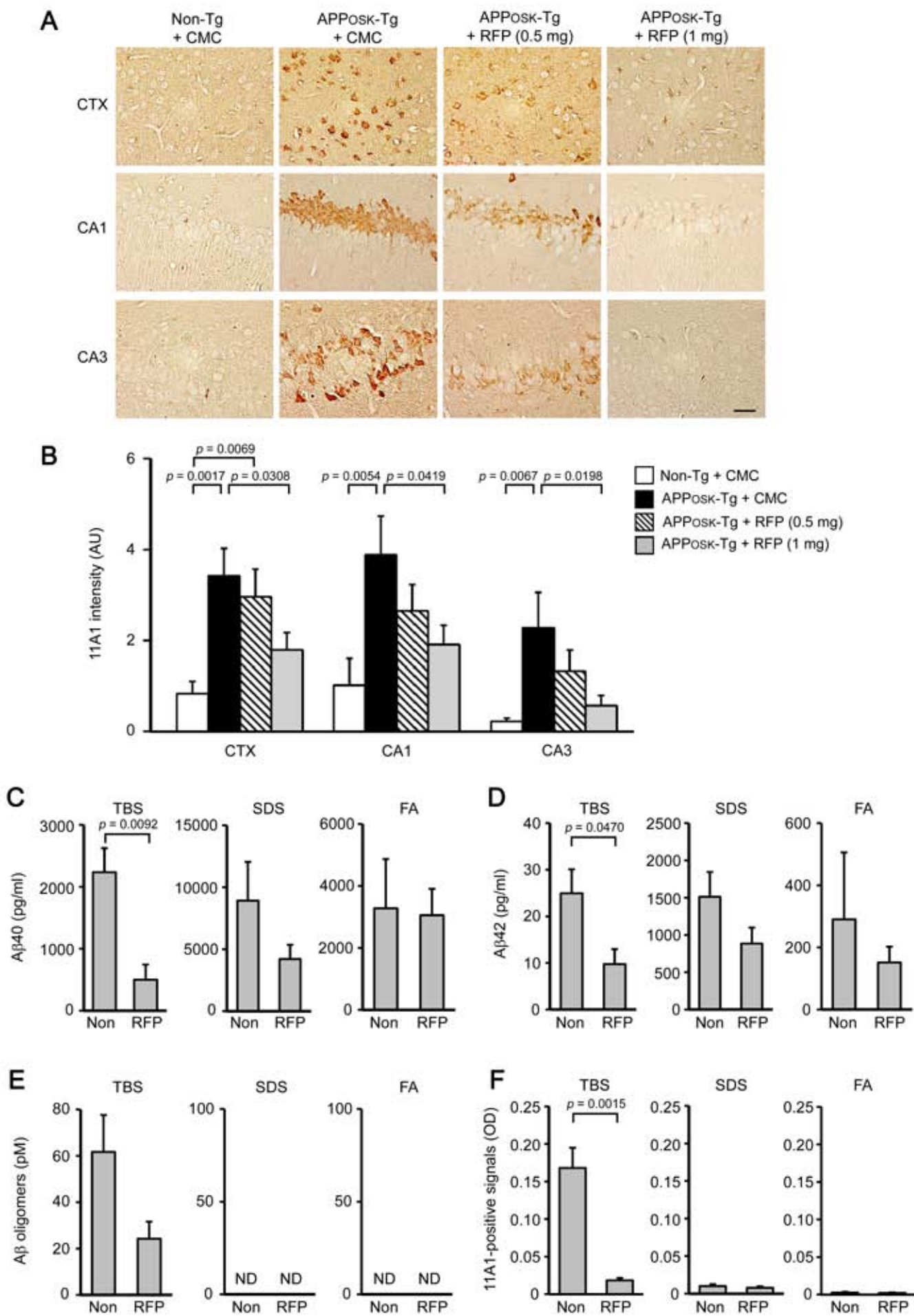


Fig. 4

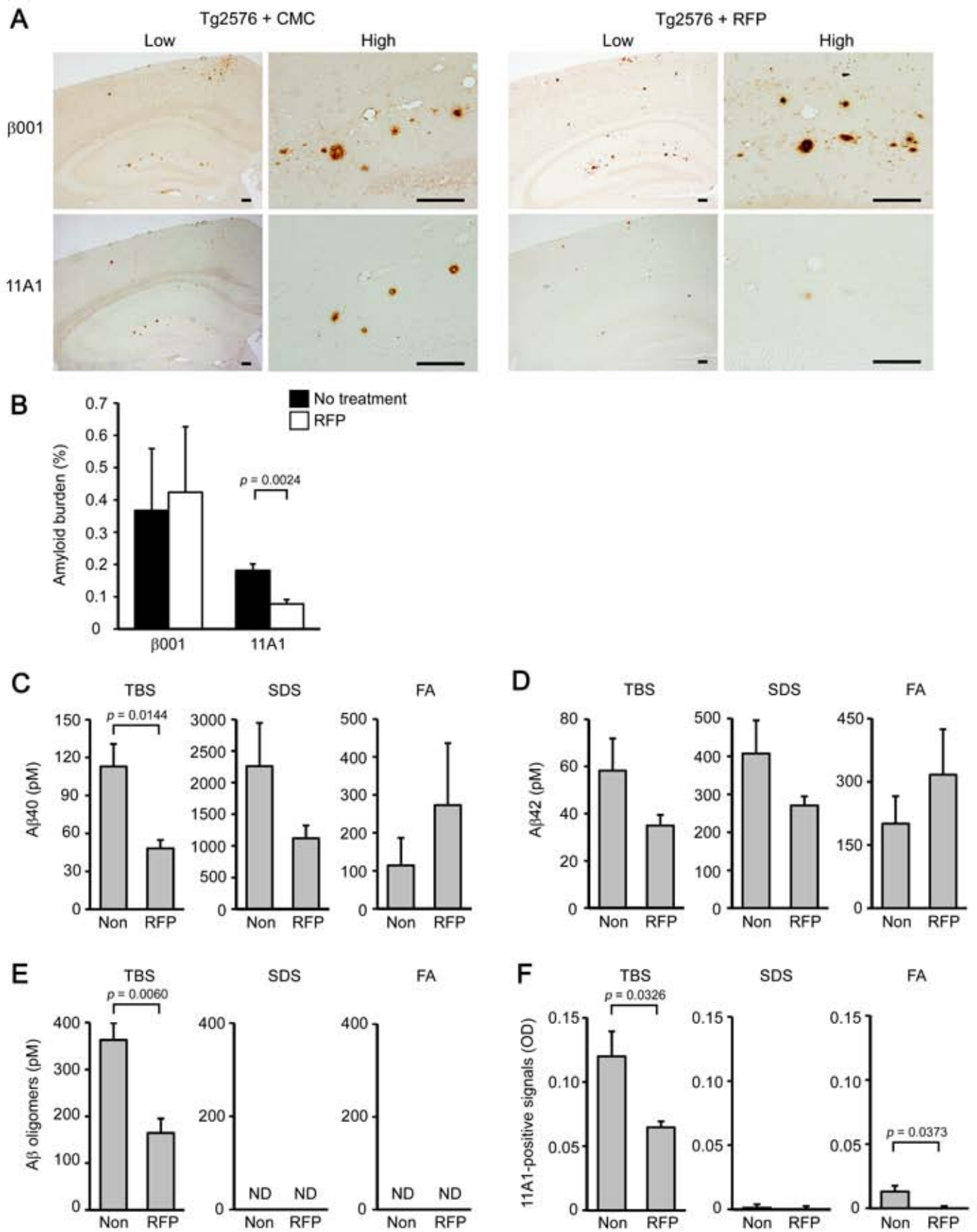


Fig. 5

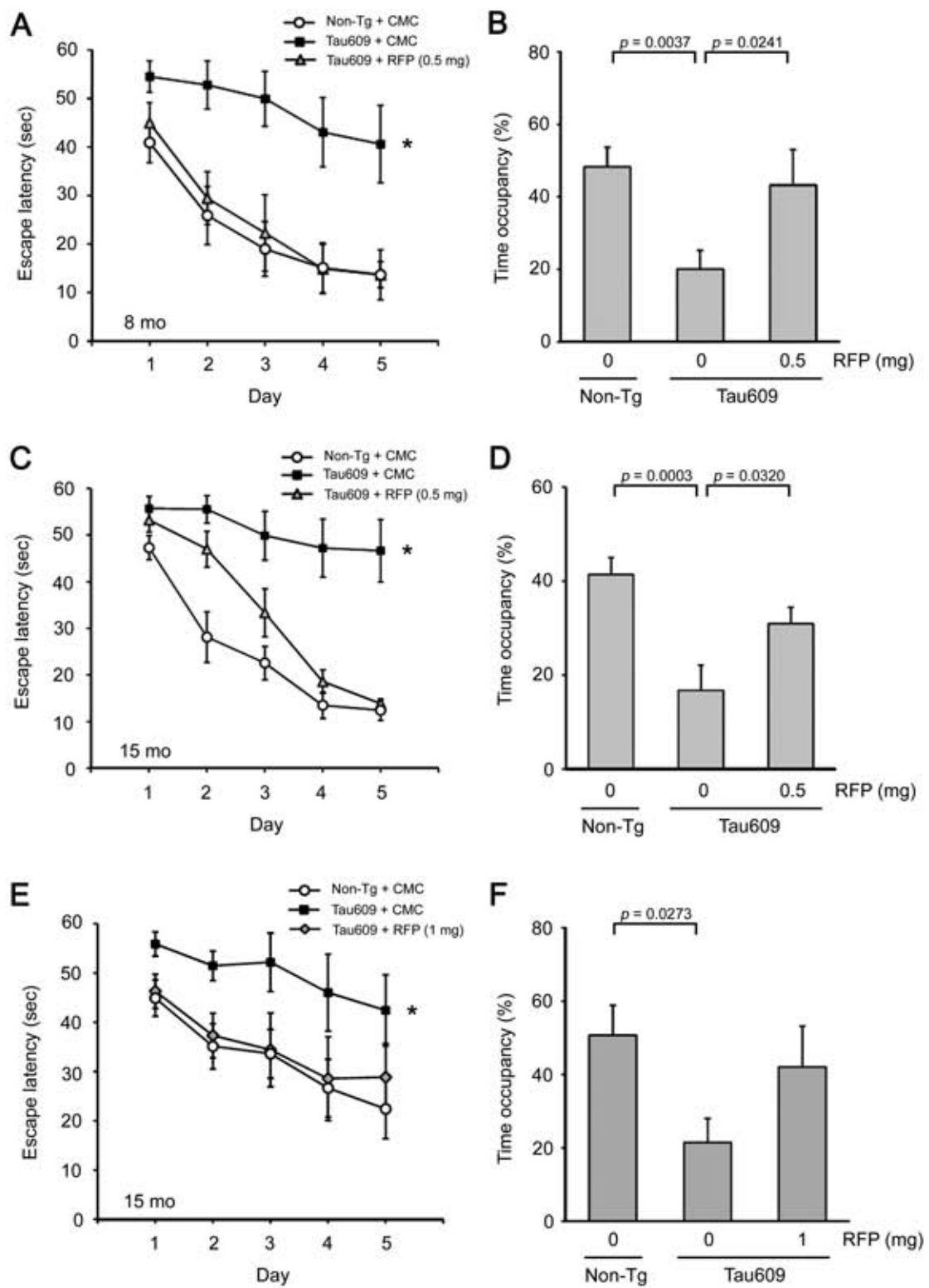


Fig. 6

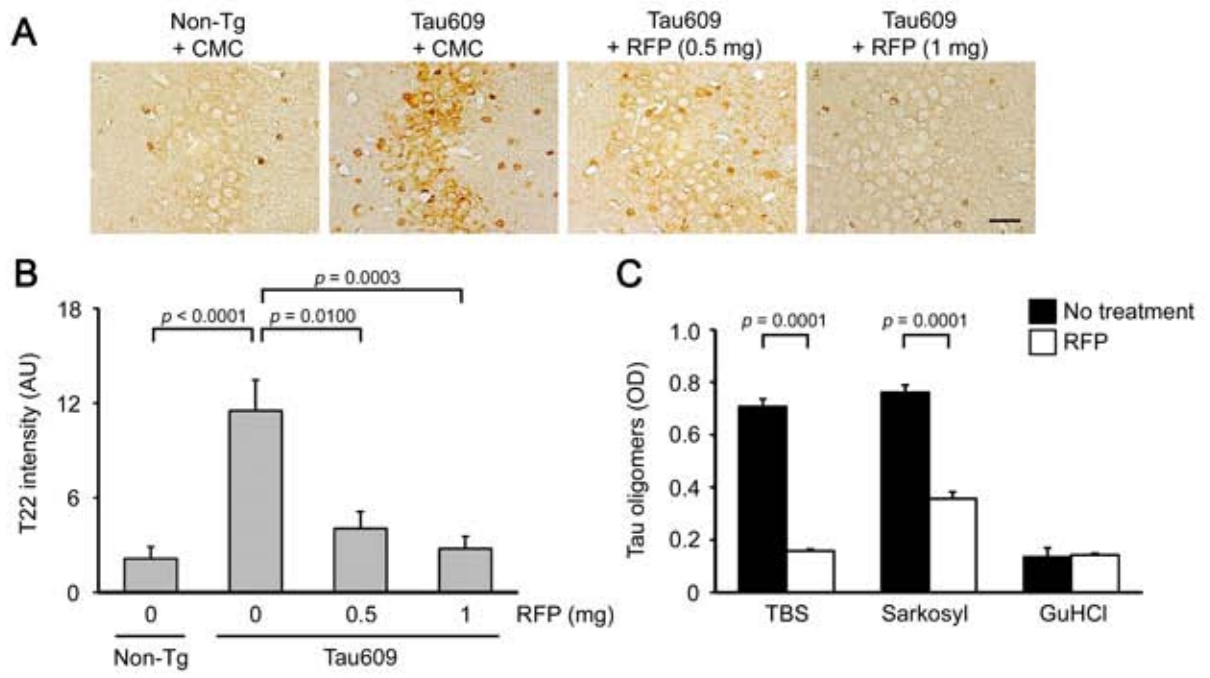


Fig. 7

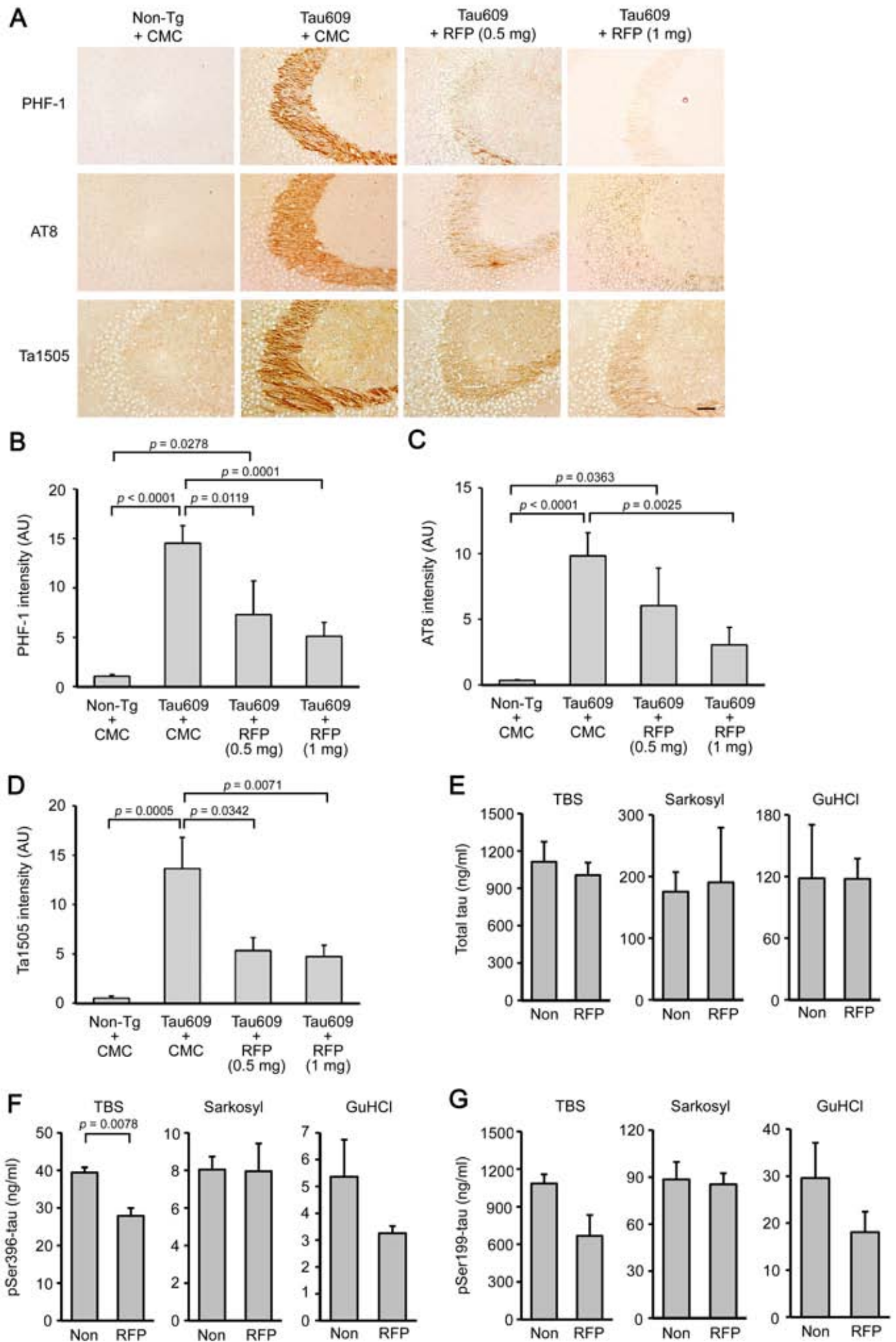
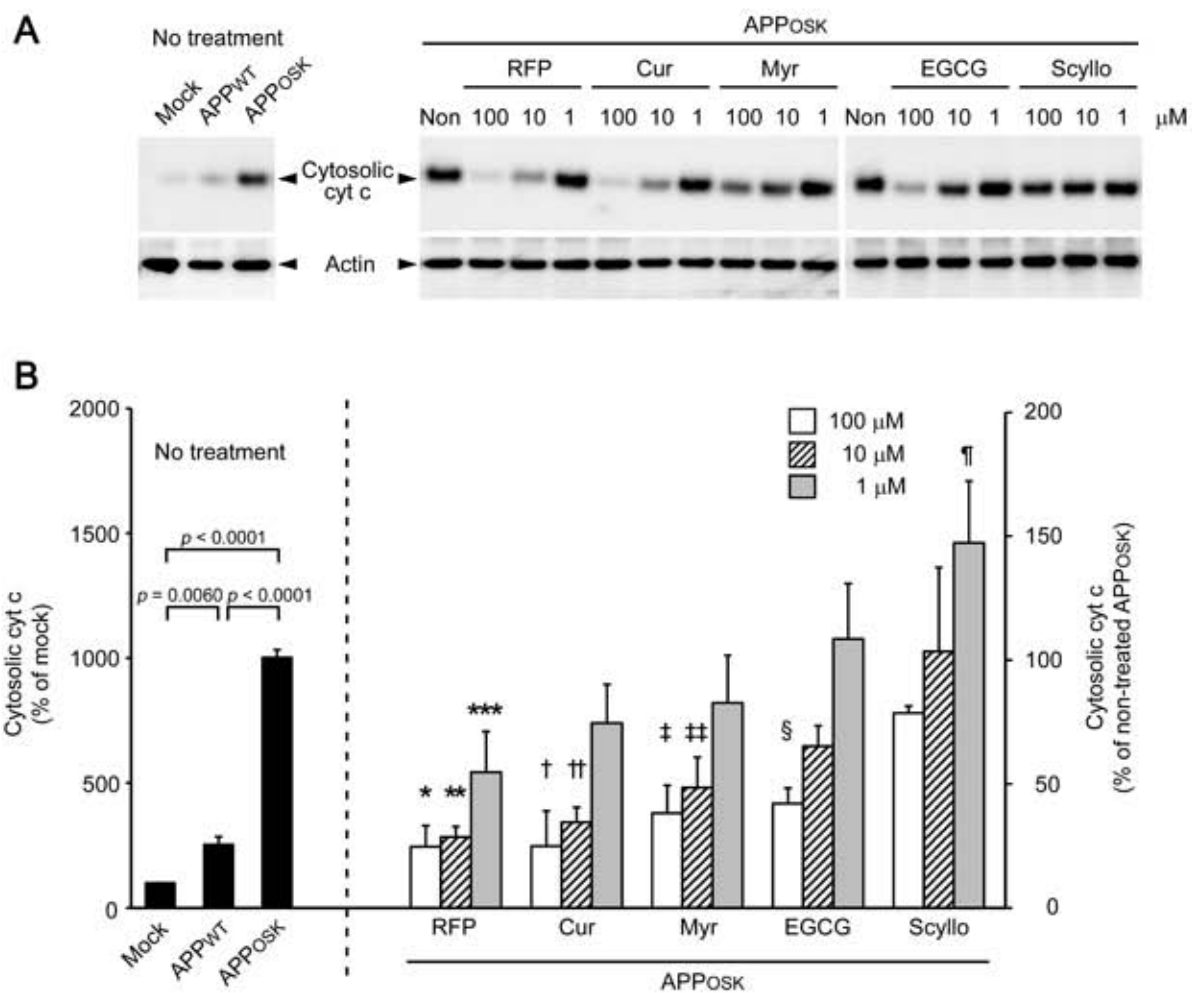
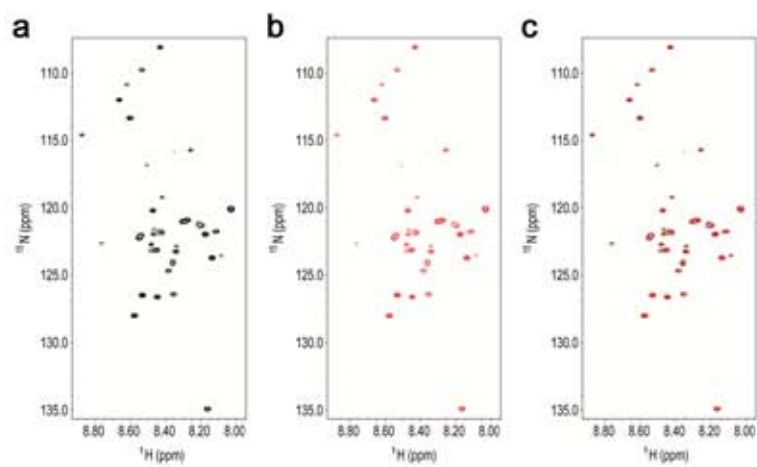


Fig. 8

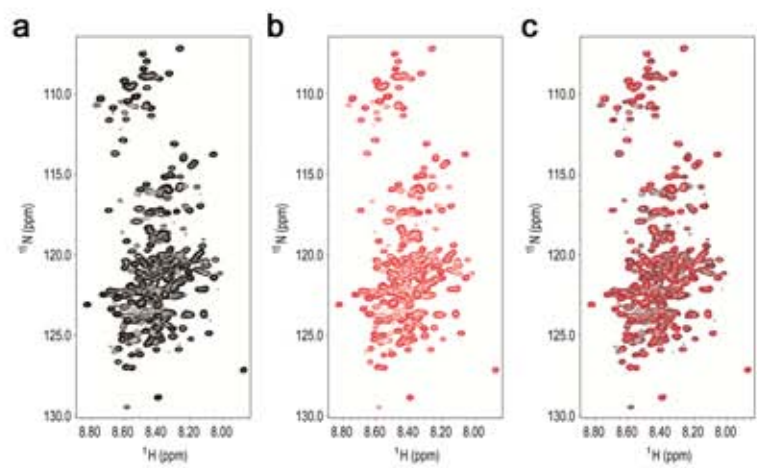


Supplementary Fig. 1

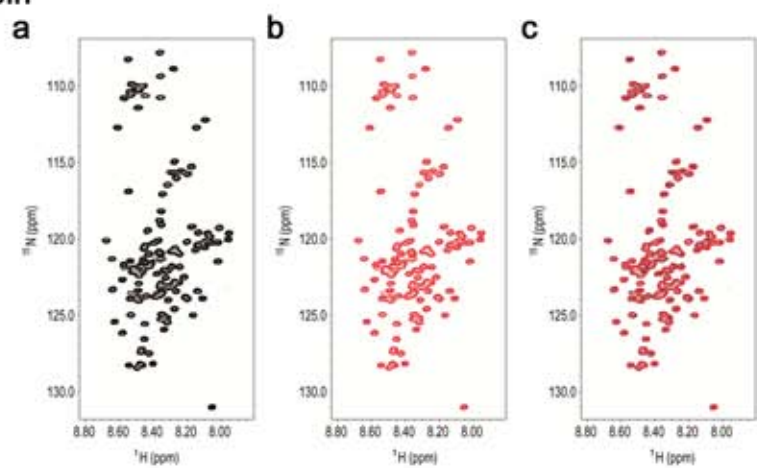
A $\text{A}\beta_{42}$



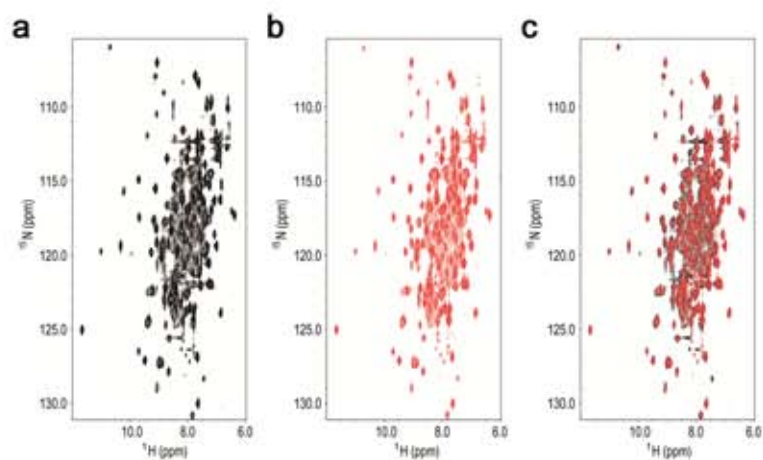
B Tau-441

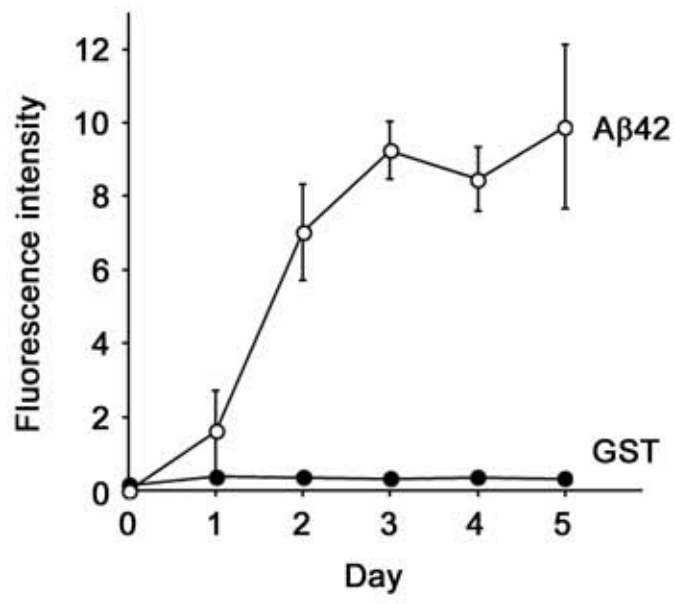


C α -Synuclein

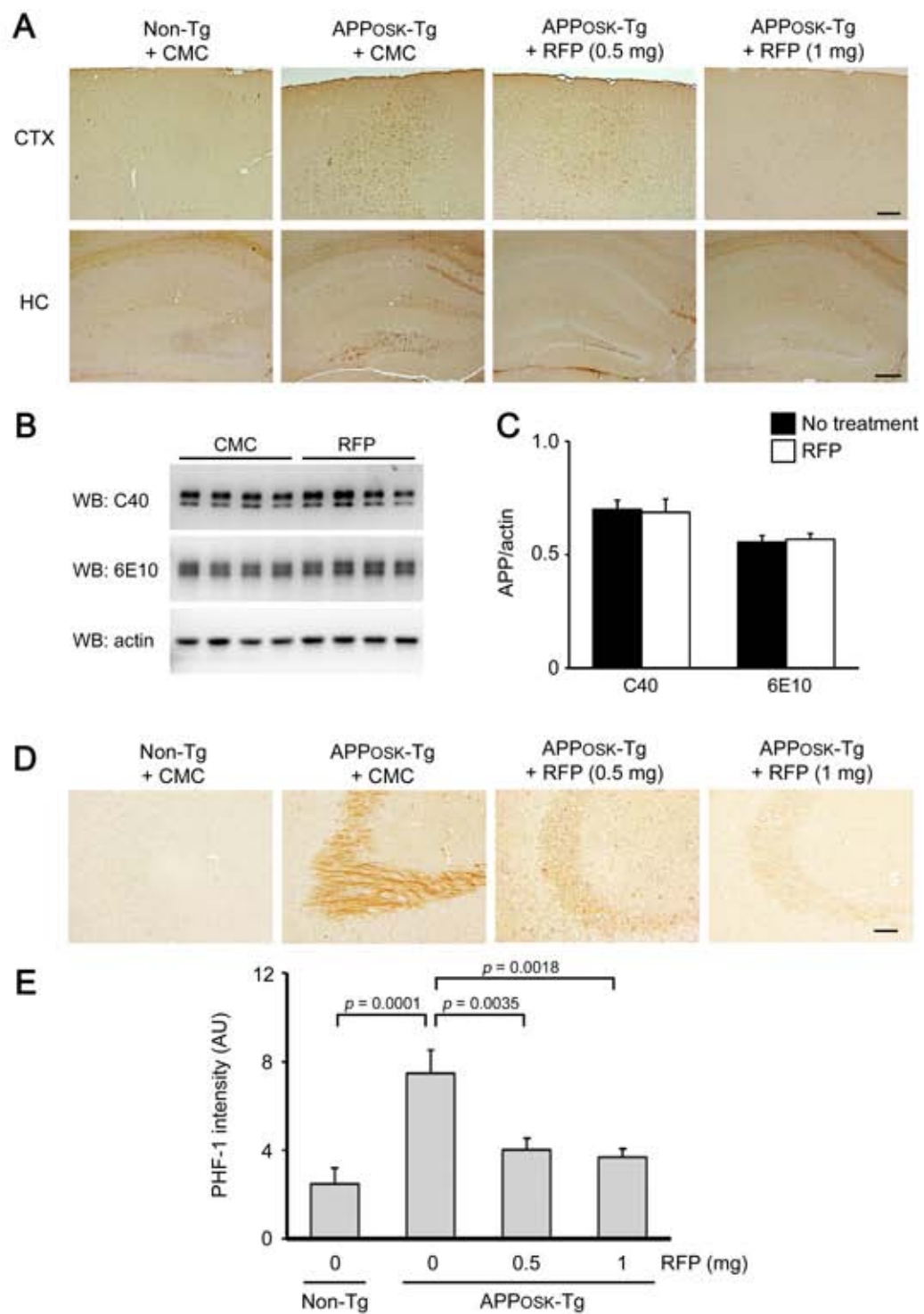


D GST

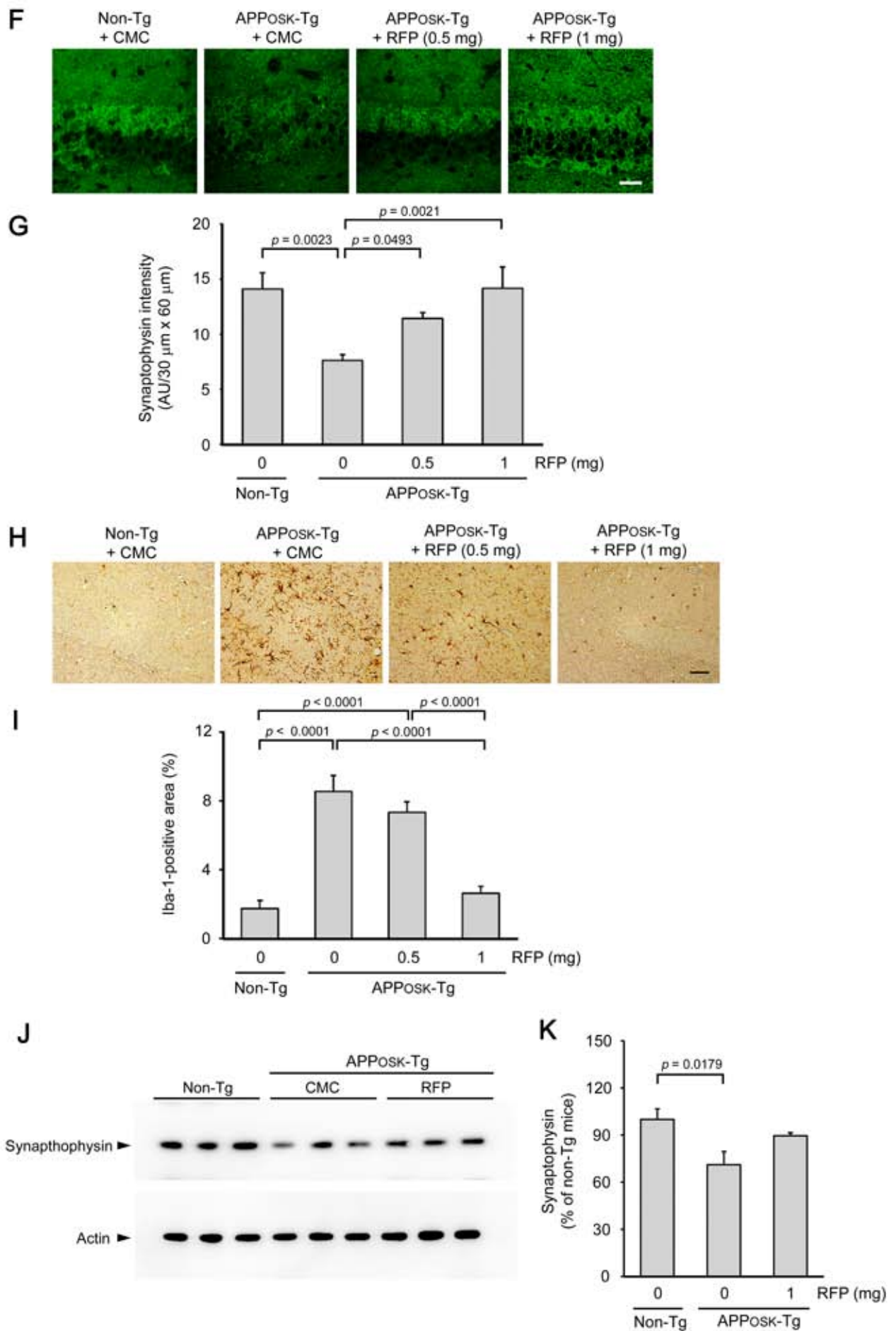




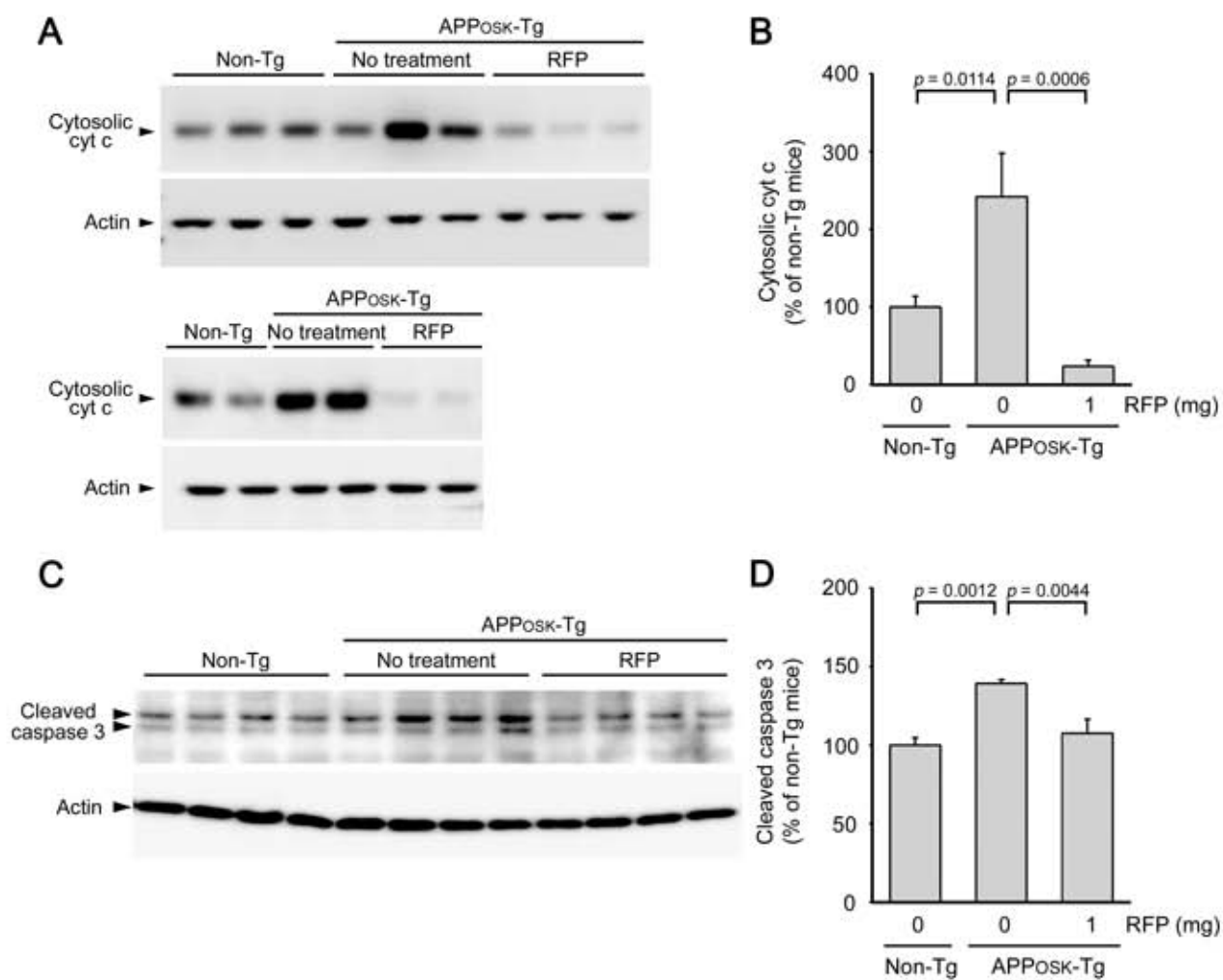
Supplementary Fig. 3



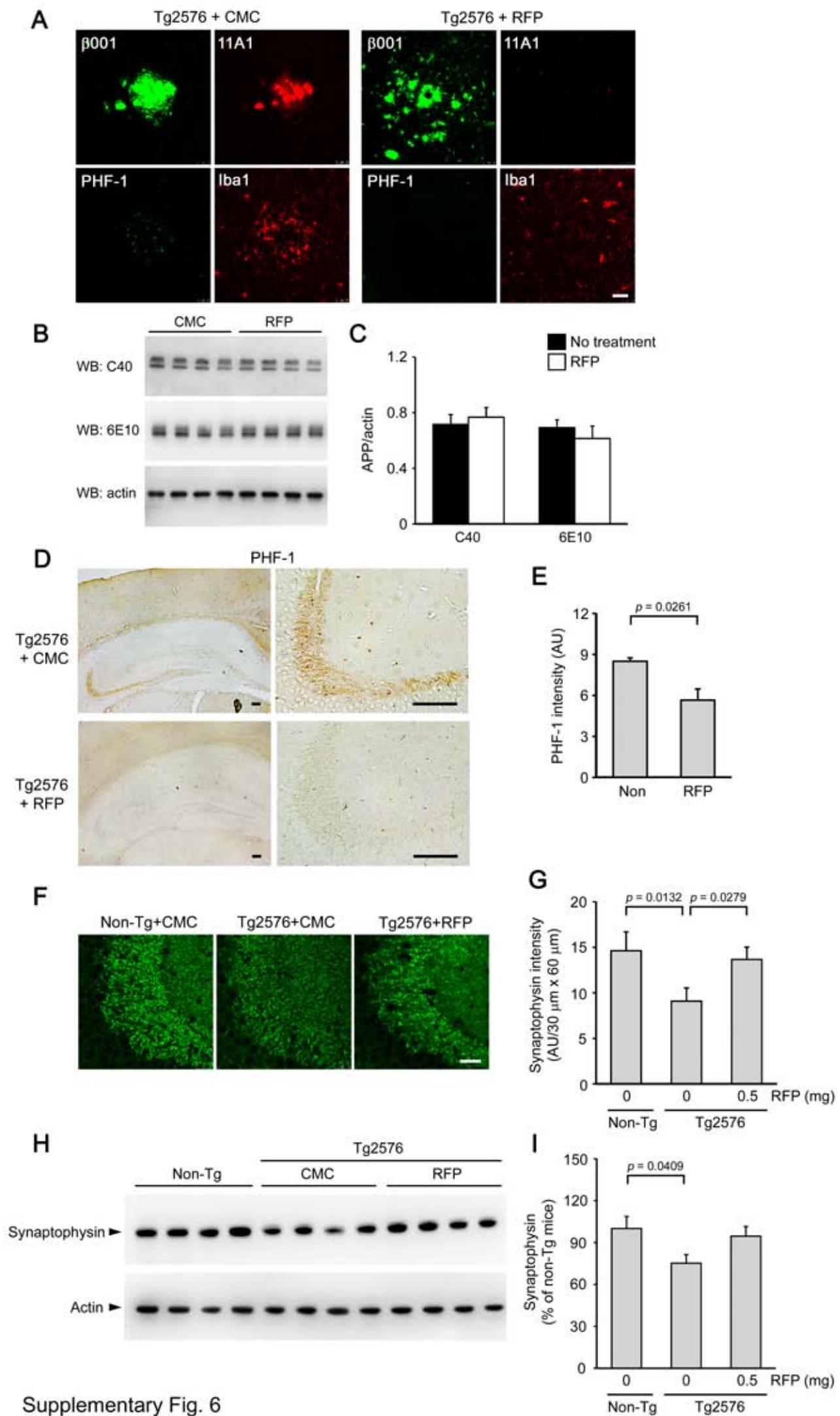
Supplementary Fig. 4



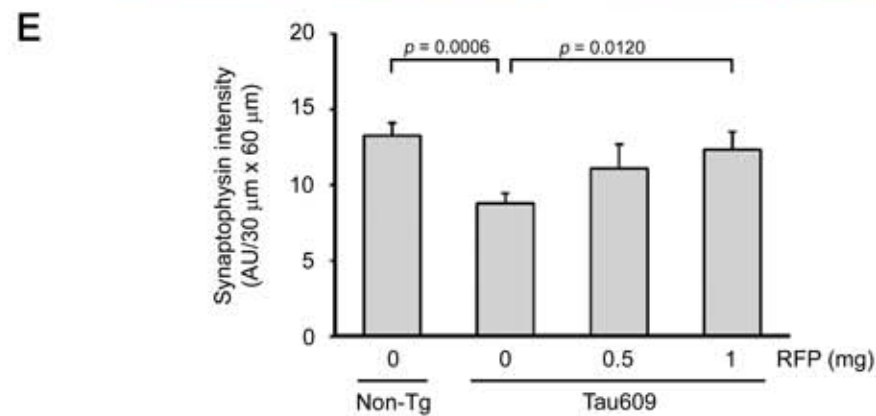
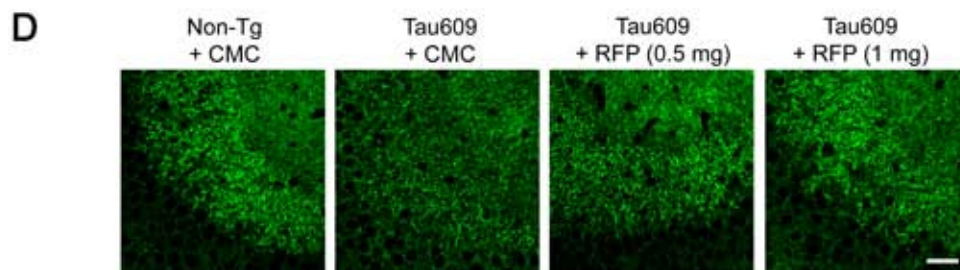
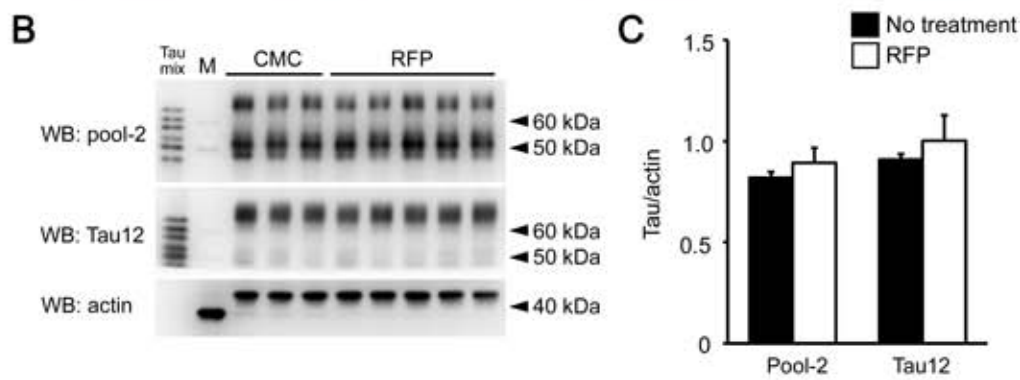
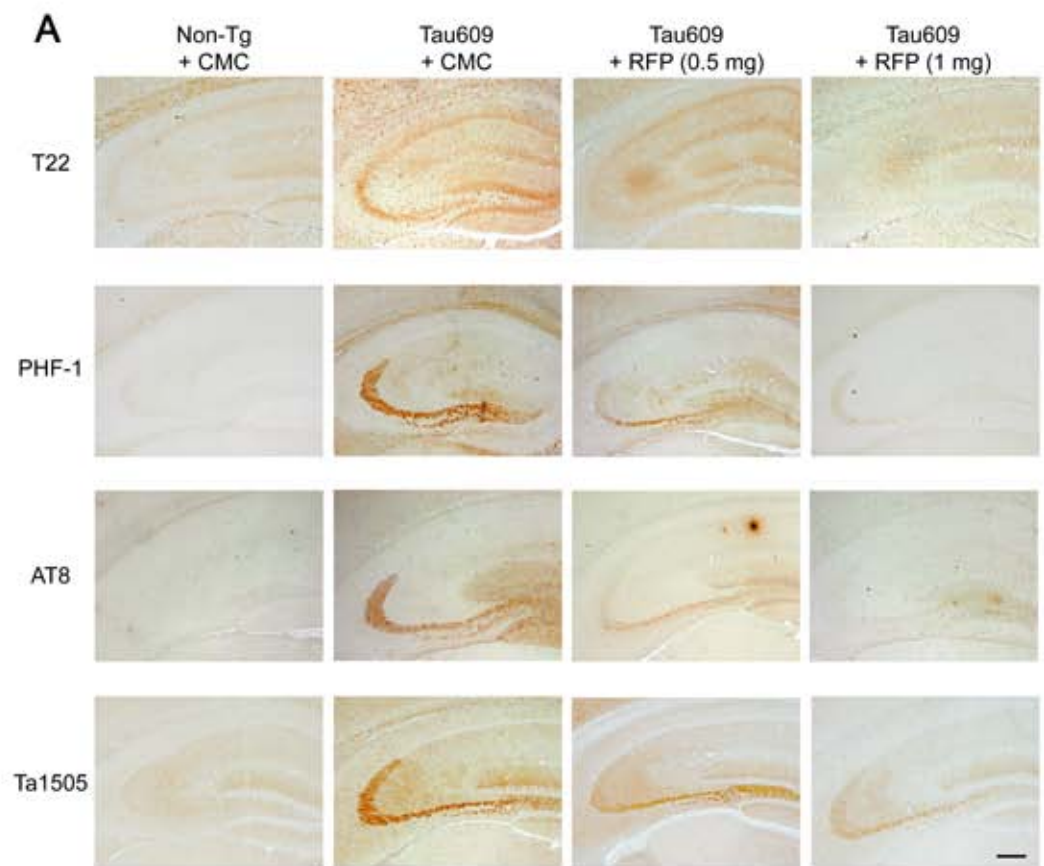
Supplementary Fig. 4 (continued)



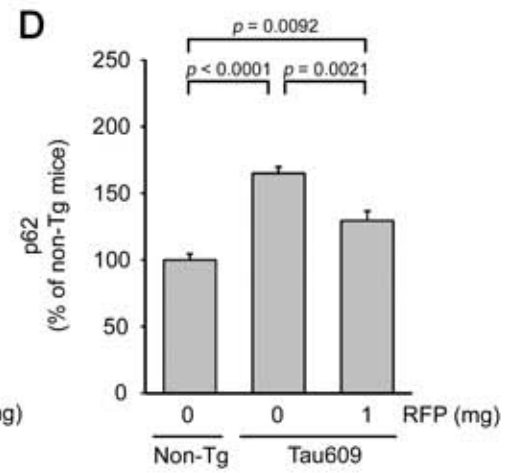
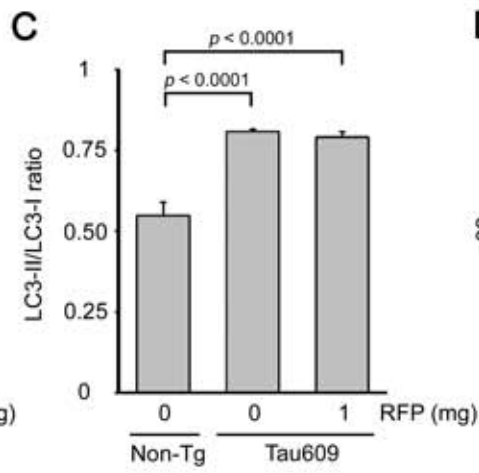
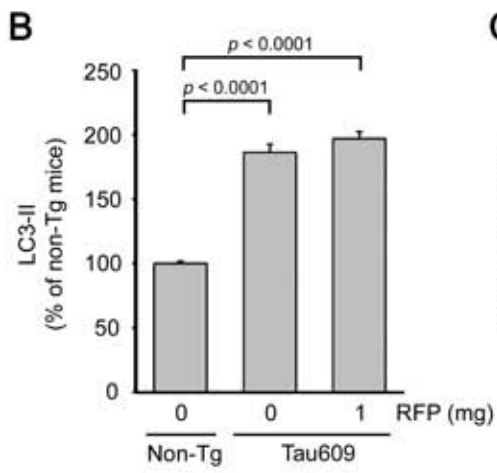
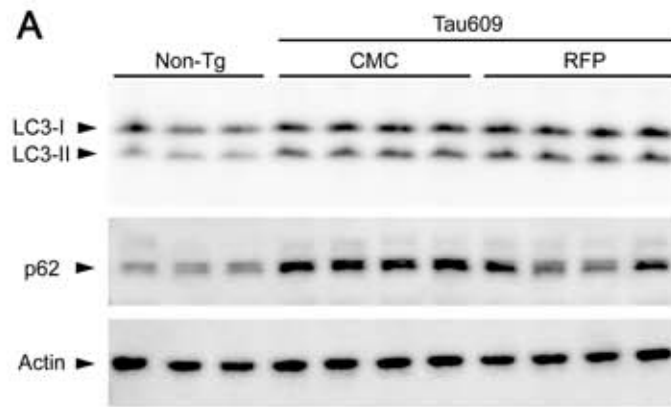
Supplementary Fig. 5



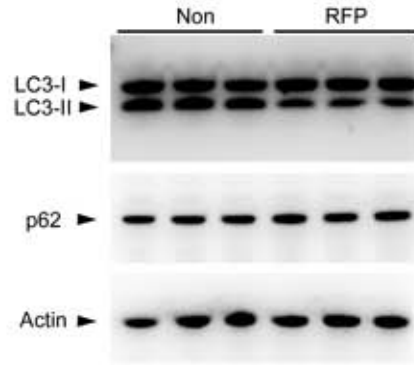
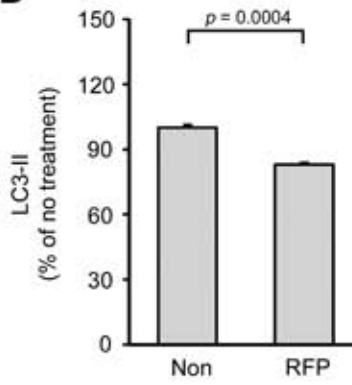
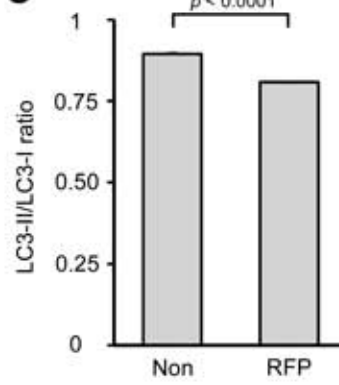
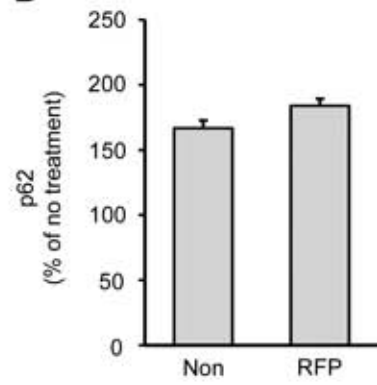
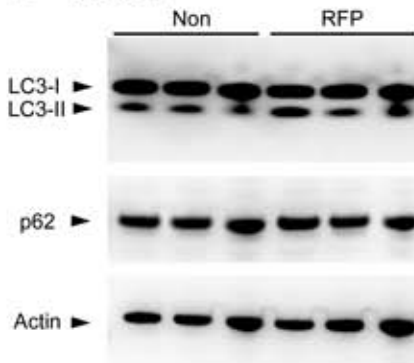
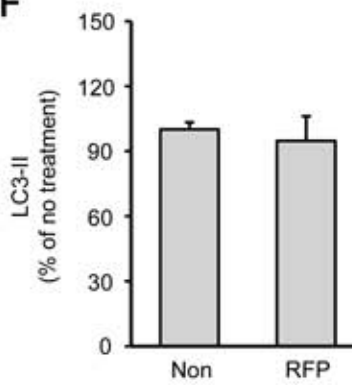
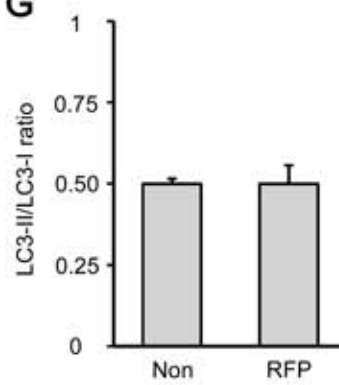
Supplementary Fig. 6



Supplementary Fig. 7



Supplementary Fig. 8

A IMR-32**B****C****D****E** COS-7**F****G****H**